PLOS ONE

RESEARCH ARTICLE

High Efficacy but Low Potency of δ-Opioid Receptor-G Protein Coupling in Brij-58-Treated, Low-Density Plasma Membrane Fragments

Lenka Roubalova[1], Miroslava Vosahlikova[1], Jana Brejchova[1], Jan Sykora[2], Vladimir Rudajev[3], Petr Svoboda[1]*

1 Department of Biomathematics, Institute of Physiology of the Czech Academy of Sciences, Prague, Czech Republic, **2** Department of Biophysical Chemistry, J. Heyrovsky Institute of Physical Chemistry of the Czech Academy of Sciences, Prague, Czech Republic, **3** Department of Neurochemistry, Institute of Physiology of the Czech Academy of Sciences, Prague, Czech Republic

* svobodap@biomed.cas.cz

OPEN ACCESS

Citation: Roubalova L, Vosahlikova M, Brejchova J, Sykora J, Rudajev V, Svoboda P (2015) High Efficacy but Low Potency of δ-Opioid Receptor-G Protein Coupling in Brij-58-Treated, Low-Density Plasma Membrane Fragments. PLoS ONE 10(8): e0135664. doi:10.1371/journal.pone.0135664

Editor: Roland Seifert, Medical School of Hannover, GERMANY

Received: September 16, 2014

Accepted: July 25, 2015

Published: August 18, 2015

Data Availability Statement: All relevant data are within the paper and its Supporting Information files.

Funding: This work was supported by the Grant Agency of the Czech Republic (P207/12/0919) and from institutional project of the Institute of Physiology, Academy of Sciences of the Czech Republic (RVO:67985823). The funders had no role in study design, data collection and analysis, decision to publish, or preparation of the manuscript.

Competing Interests: The authors have declared that no competing interests exist.

Abstract

Principal Findings

HEK293 cells stably expressing PTX-insensitive δ-opioid receptor-Gi1α ($C^{351}I$) fusion protein were homogenized, treated with low concentrations of non-ionic detergent Brij-58 at 0°C and fractionated by flotation in sucrose density gradient. In optimum range of detergent concentrations (0.025–0.05% w/v), Brij-58-treated, low-density membranes exhibited 2-3-fold higher efficacy of DADLE-stimulated, high-affinity [^{32}P]GTPase and [^{35}S]GTPγS binding than membranes of the same density prepared in the absence of detergent. The potency of agonist DADLE response was significantly decreased. At high detergent concentrations (>0.1%), the functional coupling between δ-opioid receptors and G proteins was completely diminished. The same detergent effects were measured in plasma membranes isolated from PTX-treated cells. Therefore, the effect of Brij-58 on δ-opioid receptor-G protein coupling was not restricted to the covalently bound $G_i1\alpha$ within δ-opioid receptor-$G_i1\alpha$ fusion protein, but it was also valid for PTX-sensitive G proteins of G_i/G_o family endogenously expressed in HEK293 cells. Characterization of the direct effect of Brij-58 on the hydrophobic interior of isolated plasma membranes by steady-state anisotropy of diphenylhexatriene (DPH) fluorescence indicated a marked increase of membrane fluidity. The time-resolved analysis of decay of DPH fluorescence by the "wobble in cone" model of DPH motion in the membrane indicated that the exposure to the increasing concentrations of Brij-58 led to a decreased order and higher motional freedom of the dye.

Summary

Limited perturbation of plasma membrane integrity by low concentrations of non-ionic detergent Brij-58 results in alteration of δ-OR-G protein coupling. Maximum G protein-response to agonist stimulation (efficacy) is increased; affinity of response (potency) is decreased.

The total degradation plasma membrane structure at high detergent concentrations results in diminution of functional coupling between δ-opioid receptors and G proteins.

Introduction

Membrane domains/caveolae are plasma membrane (PM) compartments enriched in cholesterol and glycosphingolipids, which are resistant to solubilization by non-ionic detergents such as Triton X-100 at 0°C [1–17]. Besides the resistance to detergent solubilization, the second characteristic feature of these PM structures is the low buoyant density when exposed to the high centrifugation force. They migrate up to the low-density area equivalent in density to 15–20% w/v sucrose. In this way, detergent-resistant membrane domains (DRMs) are separated from the bulk of plasma membranes recovered in 35% w/v sucrose. Other cell constituents remain either in "cushion solution", i.e. in the layer of highest density (40–45% w/v sucrose) or sediment down to gradient pellet (nuclear fragments).

The prototypical detergent used for preparation of DRMs is Triton X-100. The cell homogenate or membrane preparations are treated with Triton X-100 for 60 min at 0–4°C and fractionated by flotation in density gradients [7,8,18]. Unfortunately, these procedures using the high detergent concentrations (0.5–1%), result in a loss of functional coupling between GPCR and their cognate signaling molecules, trimeric G proteins and adenylyl cyclase (AC) [19]. Membrane domains/caveolae were also prepared by detergent-free method using 1M Na_2CO_3 (pH 11) and sonication [20,21], however, due to the highly alkaline pH of Na_2CO_3, the responsiveness of G proteins and AC activity to GPCR agonist stimulation was also diminished [19,22]. Isolation of the highly purified caveolae from human fibroblasts by detergent-free and alkaline-free procedure was reported by Smart et al. [23], but the amount of protein (10 μg) recovered in final preparation represented 0.13–0.14% of total protein originally present in cell homogenate (7–8 mg). Obviously, the low amount of protein in final preparation of membrane domains/caveolae is not sufficient for characterization of GPCR by radioligand binding assays using ^{3}H-labelled ligands (40–60 Ci/mmol) and measurements of G protein response to agonist stimulation by high-affinity [^{32}P]GTPase or [^{35}S]GTPγS binding assays.

Therefore, we tried to improve the methodological conditions for isolation of DRMs and tested different detergents at varying concentrations and detergent/protein ratios with the aim to prepare membrane domains with preserved functional coupling between -opioid receptors (δ-OR) and G proteins. We also tried to find some reasonable compromise between purity and amount of protein recovered in final preparation of DRMs. When using Brij-58 at low concentrations and in optimum range of protein amount in cell homogenate (10–15 mg × ml^{-1}), detergent-treated membranes floated up to the low-density end of sucrose gradient and were functional in terms of receptor-G protein coupling. Surprisingly, the efficacy of δ-OR when increasing the high-affinity [^{32}P]GTPase activity or [^{35}S]GTPγS binding was 2-3-fold higher than in membranes prepared in the absence of detergent. The potency of G protein response to agonist stimulation, however, was decreased.

Materials and Methods

Chemicals

δ-OR agonist [^{3}H]DADLE [Enkephalin (2-D-Alanine-5-D-Leucine), 50 Ci/mmol, NET 648] was purchased from PerkinElmer (Boston, MA, USA); δ-OR antagonist [^{3}H]naltrindole (60 mCi/mmol, ART0549) was from ARC (St. Louis, MO, USA). Guanosine-5′-[γ-^{35}S]

thiotriphosphate ([^{35}S]GTPγS; 1115 Ci/mmol, NEG030H) was from PerkinElmer (Boston, MA, USA); guanosine-5′-[γ-^{32}P] triophosphate ([γ^{32}P]GTP; 30 Ci/mmol, 35007) was from MP Biomedicals (Santa Ana, CA, USA). Complete protease inhibitor cocktail was from Roche Diagnostic (cat. no. 1697498, Mannheim, Germany), geneticin and hygromycin were from Life Technologies-Gibco (Paisley, Scotland). All other chemicals and drugs were purchased from Sigma-Aldrich.

Cell culture

HEK293T cells stably expressing δ-OR-$G_i1α$ ($C^{351}I$) fusion protein were cultivated in Dulbecco's modified Eagle's medium (Sigma) supplemented with 2 mM (0.292 g × l^{-1}) L-glutamine and 10% v/v newborn calf serum at 37°C as described previously [24]. Geneticin (800 μg) or hygromycin (200 μg) were included in the course of cell cultivation. The cells were grown to 80% confluency before harvesting and the beginning of experiments. When indicated, the cells were incubated with (+PTX) pertussis toxin (10 ng × ml^{-1}) for 24 h before harvesting.

Preparation of post-nuclear fraction

δ-OR-$G_i1α$ ($C^{351}I$)-HEK293 cells (δ-OR-$G_i1α$ cells for short) were harvested from 15 flasks (80 cm^2) by centrifugation for 10 min at 300 × g (0–4°C) and homogenized in 50 mM Tris-HCl, pH 7.6, 3 mM $MgCl_2$, 1 mM EDTA (TME buffer) containing 1 mM fresh PMSF plus Complete protease inhibitors cocktail in Teflon–glass homogenizer for 7 min at 1360 rpm on ice. The cell homogenate was centrifuged for 7 min at 3500 rpm (1160 × g) to separate cell debris and nuclear fraction (remaining in the sediment) from post-nuclear supernatant, PNS.

Isolation of low-density membranes (LDM) in the presence of low concentrations of non-ionic detergent Brij-58

δ-OR-$G_i1α$ ($C^{351}I$)-HEK293 cells were washed in PBS, harvested from totally 60 flasks (80 cm^2) by centrifugation for 10 min at 300 × g (0–4°C). Homogenization was performed in TME buffer containing 1 mM fresh PMSF plus Complete protease inhibitors cocktail in Teflon–glass homogenizer for 7 min at 1360 rpm on ice. The cell homogenate was divided into four identical portions having exactly the same volume. The first portion was diluted with 1/10 volume of water (no detergent). The second, third and fourth portion was diluted with 1/10 volume of water plus 10% w/v Brij-58 to a final concentration of 0.025, 0.05 and 0.1% w/v Brij-58, respectively. Exactly 2 ml volumes of these four samples were transferred into Beckman SW41 tube, mixed with 2 ml of 80% w/v sucrose, overlaid with 35%, 30%, 25%, 20% and 15% w/v sucrose (1.5 ml each) and centrifuged for 24 hours at 187,000 × g (0–4°C). Centrifugation resulted in the separation of two clearly visible layers. The lower, optically dense layer represented the plasma membrane fraction (PM). The low-density membranes (LDM) were visible as a hazy area in the upper part of sucrose gradient. Sucrose fractions 1–12 (1 ml) were collected from top to bottom of the centrifuge tube, snap frozen in liquid nitrogen and stored at -80°C.

Isolation of PM fraction in Percoll density gradient

δ-OR-$G_i1α$ ($C^{351}I$)-HEK293 cells were cultivated in 60 flasks (80 cm^2), washed in PBS and harvested by centrifugation for 10 min at 1800 rpm (300 × g) in 50 ml conical vials. The cell sediment was homogenized in 250 mM sucrose, 20 mM Tris-HCl, 3 mM $MgCl_2$, 1 mM EDTA, pH 7.6 (STEM medium) plus fresh 1 mM PMSF and protease inhibitor cocktail in loosely-fitting, Teflon-glass homogenizer for 7 min at 1360 rpm on ice. The cell homogenate was centrifuged for 7 min at 3500 rpm (1160 × g) to separate cell debris and nuclear fraction (remaining in the

sediment) from post-nuclear supernatant, PNS. A 3 ml volume of PNS was applied on the top of 20 ml of 30% v/v Percoll in thick polycarbonate Beckman Ti70 tubes. Centrifugation for 35 min at 30,000 rpm (66,200 × g) resulted in separation of two clearly visible layers. The upper layer represented the plasma membrane-enriched fraction (PM), the lower layer represented mitochondria. The upper layer was diluted 1:4 in STEM medium and centrifuged in Beckman Ti70 rotor for 1.5 hours at 50,000 rpm (175,000 × g). The PM sediment was removed from the compact, gel-like sediment of Percoll, re-homogenized by hand in a small volume of 50 mM Tris-HCl, 1 mM EDTA, pH 7.4 (TE buffer), frozen in liquid nitrogen and stored at -80°C.

[^{32}P]GTPase activity

When screening the density gradient profiles, constant volume aliquots (30 μl) of sucrose gradient fractions were incubated with or without 100 μM DADLE in reaction mix containing in a final volume of 100 μl 10 mM creatine phosphate, 5 units of creatine kinase, 0.5 μM GTP, 1 mM ATP, 0.1 mM adenosine-5′-O-(3-imidotriphosphate (App(NH)p), 1 mM ouabain, 100 mM NaCl, 5 mM $MgCl_2$, 2 mM dithiothreitol, 0.1 mM EDTA, 40 mM Tris-HCl, pH 7.5 and [γ-^{32}P]GTP (about 200,000 dpm per assay) for 30 min at 37°C. The enzyme reaction was terminated by transferring the reaction mix into the ice-cold water bath and adding 0.9 ml of 5% w/v charcoal in 10 mM phosphoric acid. After 5 min at 0°C, the charcoal was removed by centrifugation for 10 min at 10,000 × g and 0.5 ml of clear supernatant was used for determination of radioactivity by liquid scintillation.

Determination of V_{max} (GTP) and K_m (GTP) values of basal and DADLE (100 μM)-stimulated, high-affinity [^{32}P]GTPase was performed by substrate (GTP) saturation assay as described before [24,25]. [^{32}P]GTPase activity was measured as function of increasing GTP concentrations and the data expressed as Eadie-Hofstee plots. The V_{max} and K_m values were calculated by GraphPad Prism4.

Dose-response curves of agonist-stimulated [^{32}P]GTPase were measured in a 10^{-10}–10^{-3} M range of DADLE concentrations. Maximum DADLE-stimulated enzyme activity [V_{max} (DADLE)] and concentration inducing the half-maximum response [EC_{50} (DADLE)] were calculated by fitting the data by GraphPad Prism4. In all types of measurements of [^{32}P]GTPase activity, the non-specific, low-affinity [^{32}P]GTPase activity was measured in parallel assays containing 100 μM GTP and subtracted from the basal and DADLE-stimulated enzyme activity.

[^{35}S]GTPγS binding

Constant volume aliquots (20 μl) of gradient fractions were incubated in the absence (basal) or presence (agonist-stimulated) 100 μM DADLE in a final volume of 100 μl of reaction mix containing 20 mM HEPES, pH 7.4, 3 mM $MgCl_2$, 100 mM NaCl, 2 μM GDP, 0.2 mM ascorbate and [^{35}S]GTPγS (about 200,000 dpm per assay, ≈ 2nM) for 30 min at 30°C. The binding reaction was discontinued by dilution with 3 ml of ice-cold 20 mM HEPES, pH 7.4, 3 mM $MgCl_2$ and filtration through Whatman GF/C filters in Brandel cell harvester. Radioactivity remaining on the filters was determined by liquid scintillation using Rotiszint eco plus cocktail. Non-specific [^{35}S]GTPγS binding was determined in parallel assays containing 10 μM unlabeled GTPγS.

Dose-response curves of DADLE-stimulated [^{35}S]GTPγS binding were measured in a 10^{-10}–10^{-3} M range of DADLE concentrations and maximum response and EC_{50} values calculated by GraphPad Prism4. In competitive [^{35}S]GTPγS/GTPγS binding experiments, [^{35}S]GTPγS binding ± 100 μM DADLE was measured in the presence of increasing GTPγS concentrations and B_0 (GTPγS) and IC_{50} (GTPγS) values were determined by GraphPad Prism4.

[^{3}H]naltrindole binding

Post-nuclear supernatant (PNS), LDM and 0.025% Brij-58-treated LDM were incubated in TME buffer with increasing concentrations of [^{3}H]naltrindole (0.1–10.8 nM). Non-specific binding was determined in the presence of 100 μM naloxone. Binding reaction was continued for 60 min at 30°C, the bound and free radioactivity separated by filtration through GF/B filters in Brandel cell harvestor, the filters were washed three times with 3 ml ice-cold TME and the bound radioactivity was determined by liquid scintillation. Binding data were fitted with the rectangular hyperbola and K_d and B_{max} values calculated by GraphPad Prism4.

[^{3}H]DADLE binding

LDM, 0.025% Brij-58-treated LDM or Percoll-purified PM were incubated in TME buffer with increasing concentrations of [^{3}H]DADLE (0.2–39.3 nM) for 60 min at 30°C. Non-specific binding was determined in the presence of 10 μM DADLE. Separation of bound and free radioactivity was performed by filtration through Whatman GF/B filters in Brandel cell harvester, the filters were washed three times with 3 ml of ice-cold incubation buffer and radioactivity was determined by liquid scintillation. Binding data were fitted with the rectangular hyperbola and K_d and B_{max} values determined by GraphPad Prism4.

Steady-state anisotropy of fluorescence of hydrophobic membrane probe DPH

Percoll-purified PM were labeled with diphenylhexatriene (DPH) by the fast addition (under mixing) of 1 mM stock solution of DPH in freshly distilled acetone to the membrane suspension (0.1 mg protein × ml^{-1}; 1 μM final concentration); after 30 min at 25°C, which was allowed to ensure the optimum incorporation of the probe into the membrane interior [26], the anisotropy of DPH fluorescence was measured at Ex 365 nm/Em 425 nm wavelengths. Under these conditions, the fluorescence intensity of the membrane-bound DPH was ≈500x higher than that of the unbound free probe in aqueous medium; light scattering problems could be therefore omitted. Steady-state fluorescence anisotropy, r_{DPH}, was calculated according to the formula: $r_{DPH} = (I_{vv} - I_{vh})/(I_{vv} + 2I_{vh})$ as described before [27,28].

The time-resolved fluorescence and dynamic depolarization of DPH

Fluorescence lifetime and polarization experiments were performed in a time correlated single photon counting (TCSPC) spectrofluorometer IBH 5000 U equipped with a cooled Hamamatsu R3809U-50 micro-channel plate photomultiplier detector as described before [29]. The sample was excited at 373 nm with a diode laser (IBH NanoLED-375L, FWHM 80 ps, 1 MHz repetition rate). The emission monochromator was set to 450 nm with slits set to 16 nm. A 400 nm cut-off filter was placed in the emission part of the instrument to reduce a parasitic light from the laser source. The sample was continuously mixed and kept at the constant temperature of 25°C. Measurement consisted in recording of fluorescence decays at 4 different orientations of the emission and excitation polarizers. The anisotropy free decay *I (t)*, which we used for the lifetime determination, was calculated according to Eq (1):

$$I(t) = I_{vv}(t) + 2GI_{vh}(t) \quad (1)$$

where I_{vv} is the fluorescence decay measured with both excitation and emission polarized vertically, and I_{vh} with the vertically polarized excitation and horizontally polarized emission.

The G-factor (G) was determined by measuring a standard solution of POPOP and calculated according to Eq (2):

$$G = \frac{\langle I_{hv}(t)\rangle_t}{\langle I_{hh}(t)\rangle_t}, \quad (2)$$

where I_{hv} corresponds to the signal measured with the horizontally polarized excitation and vertically polarized emission, and I_{hh} to the excitation and emission both polarized horizontally. In order to obtain fluorescence lifetimes, the $I(t)$ was fitted with a two-exponential decay (Eq 3):

$$I(t) = B_1 \exp(-t/\tau_1) + B_2 \exp(-t/\tau_2), \quad (3)$$

yielding lifetimes τ_1 and τ_2 and corresponding amplitudes B_1 and B_2.

The decay of the anisotropy r(t) was determined according to Eq (4):

$$r(t) = \frac{I_{vv}(t) - GI_{vh}(t)}{I_{vv}(t) + 2GI_{vh}(t)}, \quad (4)$$

and fitted with the formula (Eq 5):

$$r(t) = (r(0) - r(\infty)).\exp(-t/\phi) + r(\infty), \quad (5)$$

where $r(0)$, and $r(\infty)$ stands for the limiting and residual anisotropy, respectively and ϕ is the rotational correlation time. The anisotropy decays were fitted by the non-linear least squares method including the impulse re-convolution with the instrumental response function (fwhm ~ 100 ps). $\chi 2$ generated by the IBH software package served as goodness of fit criterion.

The anisotropy data were analyzed according to the "wobble in cone" model introduced by [30,31]. Wobbling diffusion constant (D_w) and S-order parameter S were calculated according to Eqs 6 and 7,

$$D_w = \frac{\sigma_s}{\phi}, \quad (6)$$

$$S = \left(\frac{r(\infty)}{r(0)}\right)^{1/2}, \quad (7)$$

where $r(0)$, and $r(\infty)$ stand for limiting and residual anisotropy, ϕ is the rotational correlation time and σ_s is the relaxation time which is a function of the S-order parameter.

Protein determination

Lowry method was used for determination of protein with serum albumin (fraction V, Sigma) as protein standard. The data were calculated by fitting the calibration curve as a quadratic equation.

Results

δ-OR-G protein coupling in low-density membranes prepared from PTX-untreated δ-OR-$G_i1\alpha$ ($C^{351}I$)-HEK293 cells at 0°C; effect of non-ionic detergent Brij-58

Cell homogenate was prepared from HEK293T cells stably expressing δ-OR-$G_i1\alpha$ ($C^{351}I$) fusion protein as described in Methods and divided by volume into 4 identical parts. The three parts were treated with increasing concentrations of Brij-58 0.025%, 0.05% and 0.1% w/v, respectively; the fourth part represented the control sample of homogenate containing no

detergent. Subsequently, these 4 parts of homogenate, containing exactly the same protein concentration, were fractionated in parallel by flotation in sucrose density gradients for 24 hours and the basal and DADLE-stimulated, high-affinity [^{32}P]GTPase was measured in gradient fractions (1–12) collected from the top to bottom of the centrifuge tube as described in Methods.

The high level of total [^{32}P]GTPase activity per fraction (pmol × ml^{-1}) and specific [^{32}P] GTPase activity (pmol × min^{-1} × mg^{-1}) was detected in "floating", low-density fractions 1–6 (Fig 1). Membranes recovered in these fractions were collectively termed (in all 4 gradients) the low-density membranes, LDM. In LDM prepared in the absence of detergent (no detergent), DADLE-stimulation represented 180–240% of the basal level. In 0.025% Brij-58-treated

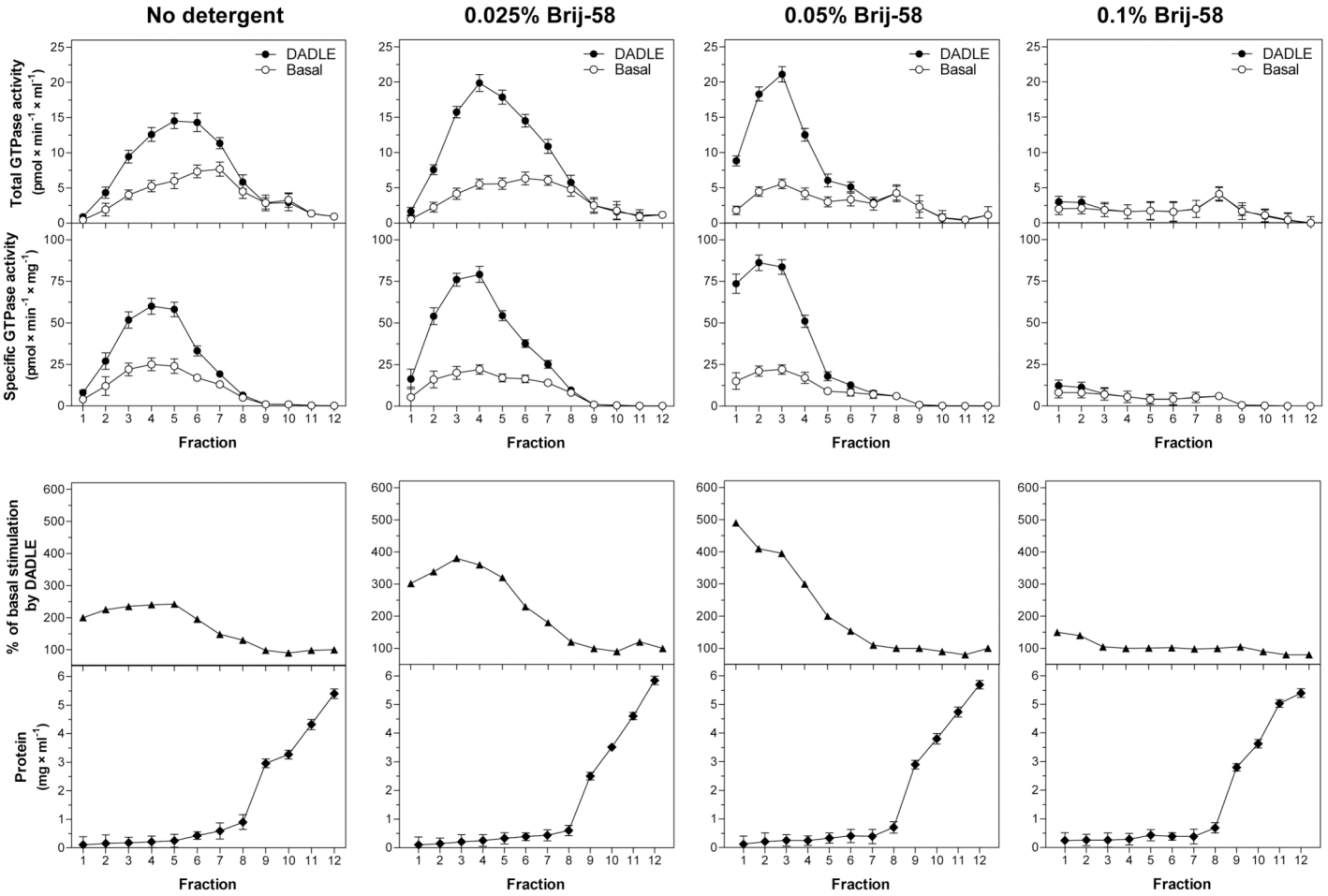

Fig 1. Subcellular fractionation of PTX-untreated δ-OR-G$_i$1α (C^{351}I)-HEK293 cells; density gradient profiles of basal and DADLE-stimulated [^{32}P] GTPase activity. Cell homogenate prepared from δ-OR-G$_i$1α cells was divided by volume into 4 identical parts. The three parts were treated with increasing concentrations of 0.025, 0.05 and 0.1% w/v Brij-58, respectively; the fourth part represented the control sample containing no detergent. Subsequently, these 4 parts of homogenate, containing exactly the same protein concentration, were fractionated by centrifugation in 15/20/25/30/35/40% w/v sucrose density gradient as described in Methods. **Upper panels.** Basal (○) and DADLE-stimulated (●), high-affinity [^{32}P]GTPase activity was measured in gradient fractions 1–12 collected from top to the bottom of the centrifuge tube and expressed as total activity (pmol × min^{-1} × ml^{-1}) or specific enzyme activity (pmol × min^{-1} × mg^{-1} protein) in each fraction. **Lower panels.** The ratio between the agonist-stimulated (DADLE) and basal level of specific enzyme activity was expressed as % of agonist stimulation over the basal level; the basal level represented 100%. The amount of protein in fractions was determined by Lowry method and expressed as mg per fraction (mg × ml^{-1}). Results represent the average of 4 experiments ± SEM. The significance of difference between the specific DADLE-stimulated and basal [^{32}P]GTPase activity in fractions 1–12 collected from sucrose density gradient 1 (no detergent), 2 (0.025% Brij-58), 3 (0.5% Brij-58) and 4 (0.1% Brij-58) was determined by Student´s t-test [see (A) in S1 Table]. Furthermore, net increment of agonist stimulation (Δ_{DADLE}) was calculated as the difference between specific DADLE-stimulated and basal [^{35}P]GTPase activity in fractions 1–6. The significance of difference of Δ_{DADLE} values in the four types of sucrose density gradients was determined by one-way ANOVA followed by Bonferroni´s multiple comparison test using GraphPad Prism4 [see (B) in S1 Table].

doi:10.1371/journal.pone.0135664.g001

LDM, agonist-stimulation was increased to 220–370%. The highest increase of DADLE stimulation (≈400%) was observed in 0.05% Brij-58-treated LDM. The further increase of detergent concentration to 0.1% was reflected in diminution of both basal and DADLE-stimulated [^{32}P]GTPase activity to the zero level (**Fig 1**, right-hand panels). Net increment of DADLE-stimulated [^{32}P]GTPase activity was also higher in 0.025% and 0.05% Brij-58-treated LDM when compared with LDM [see (B) in S1 Table].

Similar density gradient profiles were obtained by measurement of the high-affinity [^{35}S]GTPγS binding in fractions 1–12 (**Fig 2**). The 0.025% Brij-58-treated LDM recovered in low-density fractions 1–6 exhibited ≈ 2-fold higher % of DADLE stimulation over the basal level when compared with the same fractions prepared from homogenate containing no detergent,

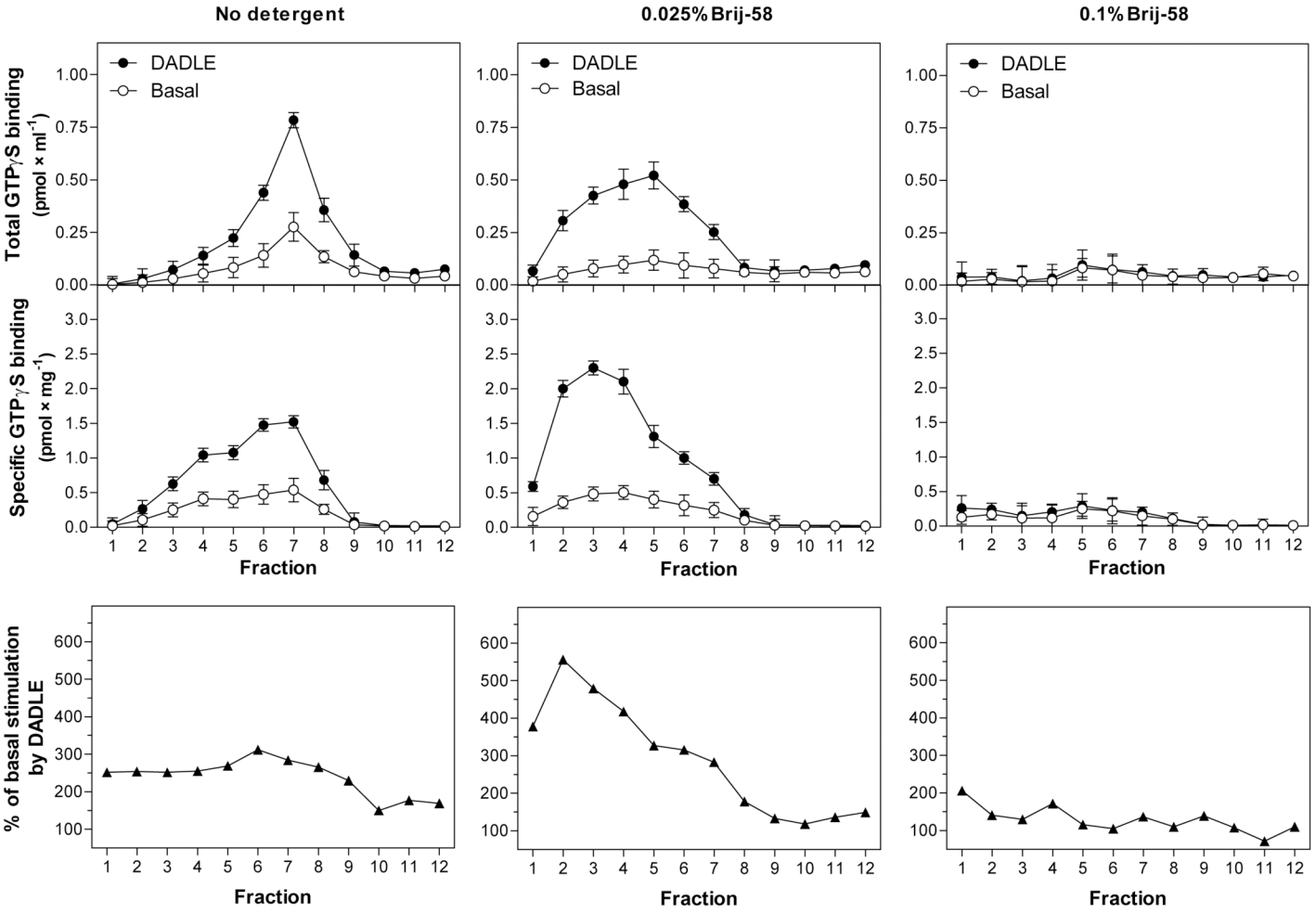

Fig 2. Subcellular fractionation of PTX-untreated δ-OR-G$_i$1α (C^{351}I)-HEK293 cells; density gradient profiles of basal and DADLE-stimulated [^{35}S]GTPγS binding. Cell homogenate prepared from δ-OR-G$_i$1α cells was divided by volume into 3 identical parts. The two parts were treated with 0.025% and 0.1% w/v Brij-58; the third part represented the control sample containing no detergent. Subsequently, these 3 parts of homogenate, containing exactly the same protein concentration, were fractionated by centrifugation in 15/20/25/30/35/40% w/v sucrose density gradients as described in Methods. **Upper panels.** Basal (○) and DADLE-stimulated (●) [^{35}S]GTPγS binding was measured in fractions 1–12 and expressed as total binding (pmol × ml^{-1}) or specific binding in each fraction (pmol × mg^{-1} protein). **Lower panels.** The ratio between the agonist-stimulated (DADLE) and the basal level of [^{35}S]GTPγS binding was calculated from specific binding data (pmol × mg^{-1} protein) and expressed as % of agonist stimulation over the basal level; the basal level represented 100%. Results represent the average of 3 experiments ± SEM. The significance of difference between the specific DADLE-stimulated and basal [^{35}S]GTPγS binding in fractions 1–12 collected from the three types of sucrose density gradients was determined by Student´s t-test [see (A) in S2 Table]. Net increment of agonist stimulation (Δ_{DADLE}) was calculated as the difference between specific DADLE-stimulated and basal [^{35}S]GTPγS binding in fractions 1–6. The significance of difference of Δ_{DADLE} values in the three types of sucrose density gradients was determined by one-way ANOVA followed by Bonferroni´s multiple comparison test using GraphPad Prism4 [see (B) in S2 Table].

doi:10.1371/journal.pone.0135664.g002

LDM. The LDM isolated from homogenate treated with 0.1% Brij-58 exhibited the zero level of both basal and DADLE-stimulated [^{35}S]GTPγS binding (Fig 2, right-hand panels). Net increment of DADLE-stimulated [^{35}S]GTPγS binding was also significantly higher in 0.025% than in LDM [see (B) in S2 Table].

Subsequently, the low-density fractions 1–6 were pooled together and the maximum enzyme activity V_{max} (GTP) and Michaelis-Menten constant K_m (GTP) of [^{32}P]GTPase reaction were determined by substrate (GTP) saturation assay (Fig 3). As before, hydrolysis of [γ-^{32}P]GTP was measured in the absence (basal) or presence of 100 μM DADLE. The maximum enzyme activity V_{max} (GTP) was increased by agonist from 42.1 ± 3.4 to 97.3 ± 3.7 pmol × min^{-1} × mg^{-1} in LDM and from 29.1 ± 2.0 to 91.5 ± 5.0 pmol × min^{-1} × mg^{-1} in 0.025% Brij-58-treated LDM (Fig 3, Table 1).

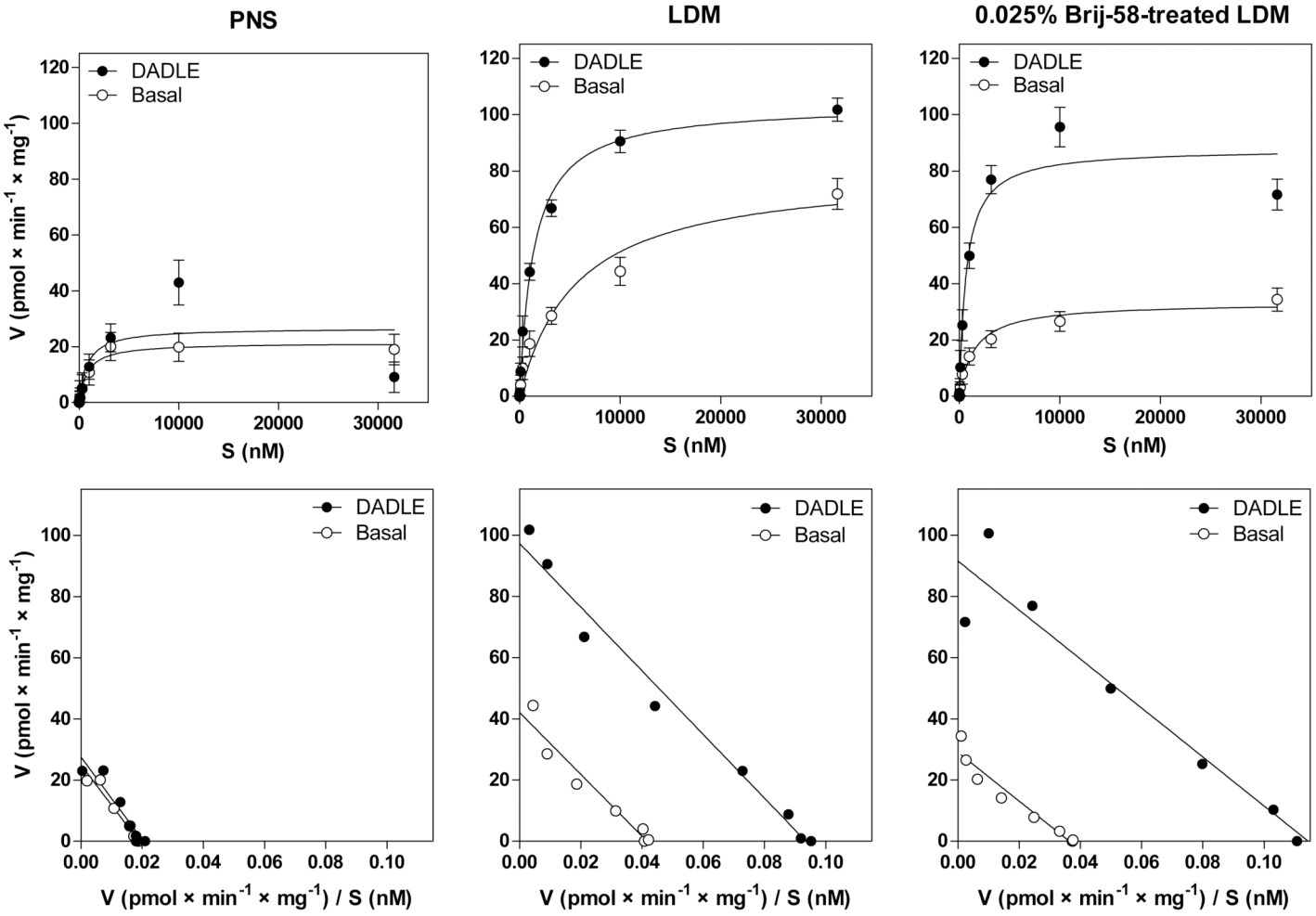

Fig 3. Basal and DADLE-stimulated [^{32}P]GTPase activity in PNS, LDM and 0.025% Brij-58-treated LDM; determination of V_{max} and K_m values. Sucrose gradient fractions 1–6 prepared by fractionation of cell homogenate prepared from δ-OR-G_i1α cells in the absence (LDM) or presence of 0.025% Brij-58 (0.025% Brij-58-treated LDM) were combined together, mixed and used for determination of basal and DADLE-stimulated [^{32}P]GTPase as described in Methods. **Upper panels**. [^{32}P]GTPase activity (pmol × min^{-1} × mg^{-1}) was measured in the absence (○) or presence (●) of 100 μM DADLE at increasing concentrations of GTP. **Lower panels.** The data were expressed as Eadie-Hofstee plots and V_{max} (GTP) and Michaelis-Menten constant K_m (GTP) calculated by GraphPad Prism4. Results represent the average of 3 experiments ± SEM. The significance of difference of V_{max} and K_m values (between the basal and DADLE-stimulated [^{32}P]GTPase) in PNS, LDM and 0.025% Brij-58-treated LDM was determined by Student´s t-test. The significance of difference of V_{max} and K_m values (for both basal and DADLE-stimulated [^{32}P]GTPase) in PNS versus LDM versus 0.025% Brij-58-treated LDM was determined by one-way ANOVA followed by Bonferroni´s multiple comparison test using GraphPad Prism4 (see S3 Table).

doi:10.1371/journal.pone.0135664.g003

Table 1. DADLE-stimulated [^{32}P]GTPase activity in membranes prepared from PTX-untreated cells; GTP saturation ± DADLE.

		PNS	LDM	0.025% Brij-58-treated LDM
V_{max}	(-DADLE)	25.0	42.1*	29.1ND
	(+DADLE)	27.5	97.3***	91.5***
Δ_{max}		2.5	55.2**	62.4**
B_{max}, [^{3}H]naltrindole		0.56	3.61*	1.74**
Δ_{max}/B_{max}		4.5	15.3*	35.9*
K_m (GTP)	(-DADLE)	1.3	1.0ND	0.8*
	(+DADLE)	1.4	1.0ND	0.8*

[^{32}P]GTPase was measured at increasing concentrations of GTP and maximum enzyme activity V_{max} (pmol × min^{-1} × mg^{-1}) and Michaelis-Menten constant K_m (nM) were calculated from Eadie-Hofstee plots presented in lower panels of Fig 3. Net increment of DADLE-stimulation **(Δ_{max})** was determined as the difference between V_{max} (+DADLE) and V_{max} (-DADLE). B_{max}, number of [^{3}H]naltrindole binding sites (pmol × mg^{-1}); Δ_{max}/B_{max} ratio, Δ_{max} normalized to receptor number.

* ($p<0.05$)

** ($p<0.01$)

*** ($p<0.001$) indicates a significant difference between PNS and LDM (no detergent) or between PNS and 0.025% Brij-58-treated LDM; ND ($p>0.05$), not different.

doi:10.1371/journal.pone.0135664.t001

The net increment of agonist stimulation Δ_{max}, calculated as the difference between V_{max} of DADLE-stimulated (+DADLE) and V_{max} of basal level (-DADLE) of [^{32}P]GTPase activity was in LDM 22-fold higher than in post-nuclear fraction (PNS); in Brij-58-treated LDM, Δ_{max} was 25-fold higher than in PNS (Table 1). Thus, the significant purification of δ-OR-G_i1α ($C^{351}I$) fusion protein in both preparations of LDM was obtained. Determination of K_m values in PNS ± DADLE (1.3 ± 0.1 and 1.4 ± 0.2 μM), in LDM ± DADLE (1.0 ± 0.1 and 1.0 ± 0.1 μM) and in 0.025% Brij-58-treated LDM ± DADLE (0.8 ± 0.1 and 0.8 ± 0.1 μM) indicated the same affinity of [^{32}P]GTPase to its substrate and no change by an agonist.

The results of measurement of maximum enzyme activity ± DADLE described in the previous paragraph were supported by comparison of the dose-response curves of DADLE-stimulated [^{32}P]GTPase in PNS, LDM and 0.025% Brij-58-treated LDM (Fig 4). DADLE-stimulated [^{32}P]GTPase measured at saturating concentration of agonist (v_{DADLE}) was substantially increased by purification of LDM: the net increment of agonist stimulation (Δ_{DADLE}) was increased from 3.1 ± 0.3 pmol × min^{-1} × mg^{-1} in PNS to 15.4 ± 0.5 pmol × min^{-1} × mg^{-1} in LDM. In 0.025% Brij-58-treated LDM, Δ_{DADLE} (20.9 ± 0.7 pmol × min^{-1} × mg^{-1}) was 7-fold higher than in PNS (Fig 4, upper panels). However, the potency of [^{32}P]GTPase activation by DADLE, expressed as the agonist concentration inducing the half-maximum response (EC_{50}), was decreased by one order of magnitude in 0.025% Brij-58-treated LDM (EC_{50} = 420.8 ± 2.0 nM) when compared with LDM (EC_{50} = 44.4 ± 2.1 nM) or PNS (35.3 ± 2.0 nM) (Fig 4 and Table 2).

The significant increase of purity of δ-OR-G_i1α in LDM and Brij-58-treated LDM, which was, in the case of Brij-58-treated LDM, accompanied by a decrease of potency of G protein response (5-fold), was also detected by comparison of the dose-response curves of DADLE-stimulated [^{35}S]GTPγS binding (Fig 5, Table 3). The net increment of agonist stimulation in LDM (Δ_{DADLE} = 0.56 ± 0.07 pmol × mg^{-1}) and 0.025% Brij-58-treated LDM (Δ_{DADLE} = 0.93 ± 0.08 pmol × mg^{-1}) was 6- and 9-fold higher than in PNS (0.10 ± 0.05 pmol × mg^{-1}). As before, EC_{50} values were not significantly different when compared in PNS (19.1 ± 1.3 nM) and LDM (15.4 ± 1.4 nM), but significantly increased in Brij-58-treated LDM (EC_{50} = 81.5 ± 3.4 nM). Thus, the lower potency of agonist response in Brij-58-treated LDM was

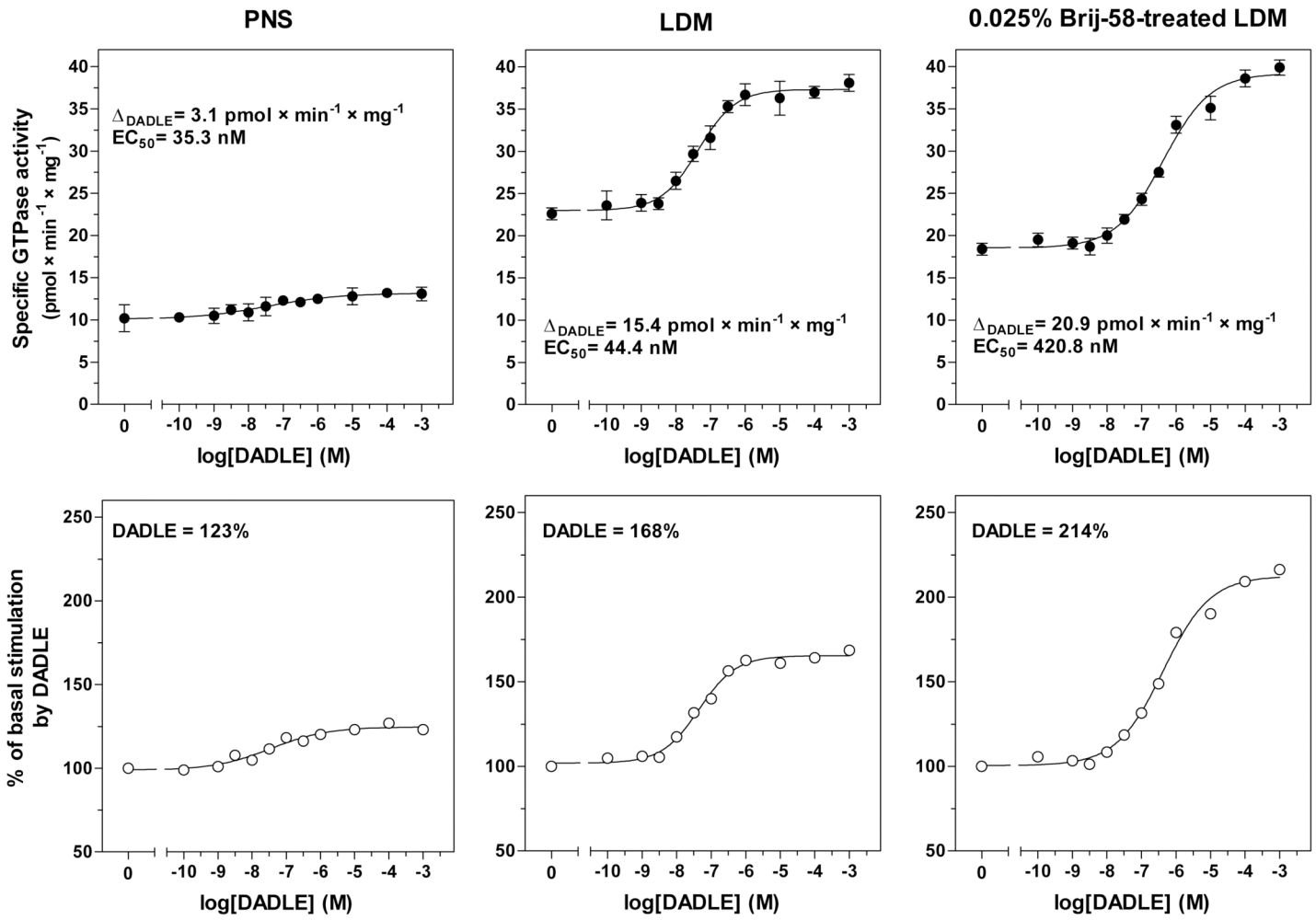

Fig 4. Dose-response curves of DADLE-stimulated [^{32}P]GTPase; comparison of PNS, LDM and 0.025% Brij-58-treated LDM. Upper panels. Dose-response curves of DADLE-stimulated [^{32}P]GTPase were measured in post-nuclear supernatant (PNS), low-density membranes (LDM) and 0.025% Brij-58-treated LDM prepared from δ-OR-G_i1α cells as described in Methods. LDM and 0.025% Brij-58-treated LDM represent the mixed pool of membranes in combined fractions 1–6 prepared in the absence or presence of detergent, respectively. The net increment of agonist-stimulation (Δ_{DADLE}) and DADLE concentration inducing the half-maximum response (EC_{50}) were calculated by GraphPad Prism4. **Lower panels.** The ratio between the agonist-stimulated (DADLE) and basal level of specific enzyme activity was expressed as % of agonist stimulation over the basal level; the basal level represented 100%. Results represent the average of 3 experiments ± SEM. The significance of difference of EC_{50} and Δ_{DADLE} in PNS versus LDM versus 0.025% Brij-58-treated LDM was determined by one-way ANOVA followed by Bonferroni´s multiple comparison test using GraphPad Prism4 (see S4 Table).

doi:10.1371/journal.pone.0135664.g004

noticed by measurement of both DADLE-stimulated, high-affinity [^{32}P]GTPase (Fig 4) and [^{35}S]GTPγS binding (Fig 5).

In the following step of our work, PNS, LDM and 0.025% Brij-58-treated LDM were compared by measurement of [^{35}S]GTPγS/GTPγS competitive inhibition curves determined in the presence or absence of 100 μM DADLE (Fig 6). Purification of LDM by flotation in sucrose gradient and increase of efficacy by detergent was documented again. The DADLE-stimulated [^{35}S]GTPγS binding level at zero concentration of GTPγS (B_0), was increased from 0.22 ± 0.01 pmol × mg^{-1} in PNS to 1.08 ± 0.02 and 1.19 ± 0.02 pmol × mg^{-1} in LDM and 0.025% Brij-58-treated LDM, respectively. The net increment of agonist stimulation (ΔB_0), calculated as the difference between B_0 (+DADLE) and B_0 (—DADLE), was increased from 0.11 ± 0.01 pmol × mg^{-1} in PNS to 0.61 ± 0.03 pmol × mg^{-1} and 0.98 ± 0.02 pmol × mg^{-1} in LDM and Brij-58-treated LDM, respectively (Table 4). Comparison of IC_{50} values in PNS, LDM and

Table 2. DADLE-stimulated [^{32}P]GTPase activity in membranes prepared from PTX-untreated cells; dose-response curves.

	PNS	LDM	0.025% Brij-58-treated LDM
Δ_{DADLE}	3.1	15.4*	20.9**
Δ_{DADLE}/B_{max}	5.5	4.3ND	12.0*
EC_{50}	35.3	44.4ND	420.8***

[^{32}P]GTPase activity was measured in the absence (V_{basal}) or presence (V_{DADLE}) of increasing concentrations of DADLE (Fig 4). Δ_{DADLE}, net increment of agonist stimulation, was calculated as the difference between V_{DADLE} at saturating concentration and V_{basal}; Δ_{DADLE}/B_{max} ratio, Δ_{DADLE} normalized to receptor number; EC_{50} (nM); DADLE concentration inducing half-maximum stimulation of [^{32}P]GTPase activity.

* ($p<0.05$)

** ($p<0.01$)

*** ($p<0.001$) indicates a significant difference between PNS and LDM (no detergent) or between PNS and 0.025% Brij-58-treated LDM; ND ($p>0.05$), not different.

doi:10.1371/journal.pone.0135664.t002

Brij-58-treated LDM indicated no significant difference between the three types of membranes in this type of experiment (Fig 6).

We have also determined the number of δ-opioid receptors in PNS, LDM and 0.025% Brij-58-treated LDM by saturation binding assay with antagonist [^{3}H]naltrindole (Fig 7). As before, purification of δ-OR-$G_i1\alpha$ protein was evidenced again because B_{max} of [^{3}H]naltrindole binding in LDM (3.61 ± 0.21 pmol × mg^{-1}) was 7-fold higher than in PNS (0.56 ± 0.21 pmol × mg^{-1}). However, in 0.025% Brij-58-treated LDM, number of receptor sites was less than half of this amount ($B_{max} = 1.74 \pm 0.11$ pmol × mg^{-1}). This result may be interpreted as the detergent-induced loss of approximately half of membrane bound δ-OR. The affinity of [^{3}H]naltrindole binding was unchanged by detergent treatment.

The B_{max} values of [^{3}H]naltrindole binding were subsequently used for normalization of [^{32}P]GTPase results according to the number of receptors present in a given membrane preparation. Calculation of Δ_{max}/B_{max} and Δ_{DADLE}/B_{max} ratios in Brij-58-treated LDM indicated 2.4- and 2.8-fold higher values than in LDM (**Tables 1 and 2**). Similar ratios were obtained by normalization of [^{35}S]GTPγS binding data: Δ_{DADLE}/B_{max} and $\Delta B_0/B_{max}$ ratios were 3.3-fold higher in Brij-58-treated LDM than in LDM (**Tables 3 and 4**). These results may be simply interpreted as a loss of about half of receptor sites in 0.025% Brij-58-treated LDM when compared with LDM.

It may be therefore concluded that Brij-58-treated LDM prepared at a low detergent concentrations exhibit the high efficacy when activating their cognate G proteins, but the affinity of agonist response, expressed as EC_{50} values of DADLE-stimulated [^{32}P]GTPase or [^{35}S]GTPγS binding, is decreased by one order of magnitude.

δ-OR-G protein coupling in low-density membranes prepared from PTX-treated δ-OR-$G_i1\alpha$ ($C^{351}I$)-HEK293 cells at 0°C; effect of non-ionic detergent Brij-58

Virtually the same results were obtained in analysis of 0.025% Brij-58-treated membranes prepared from δ-OR-$G_i1\alpha$ cells exposed to pertussis toxin (10 ng × ml^{-1}) for 12 hours. The screening of density gradient profiles indicated that the peak of DADLE-stimulated [^{35}S]GTPγS binding was shifted to lower densities: from fractions 5+6, which were combined together and corresponded to plasma membrane fractions, to fraction 4. The net increment of agonist

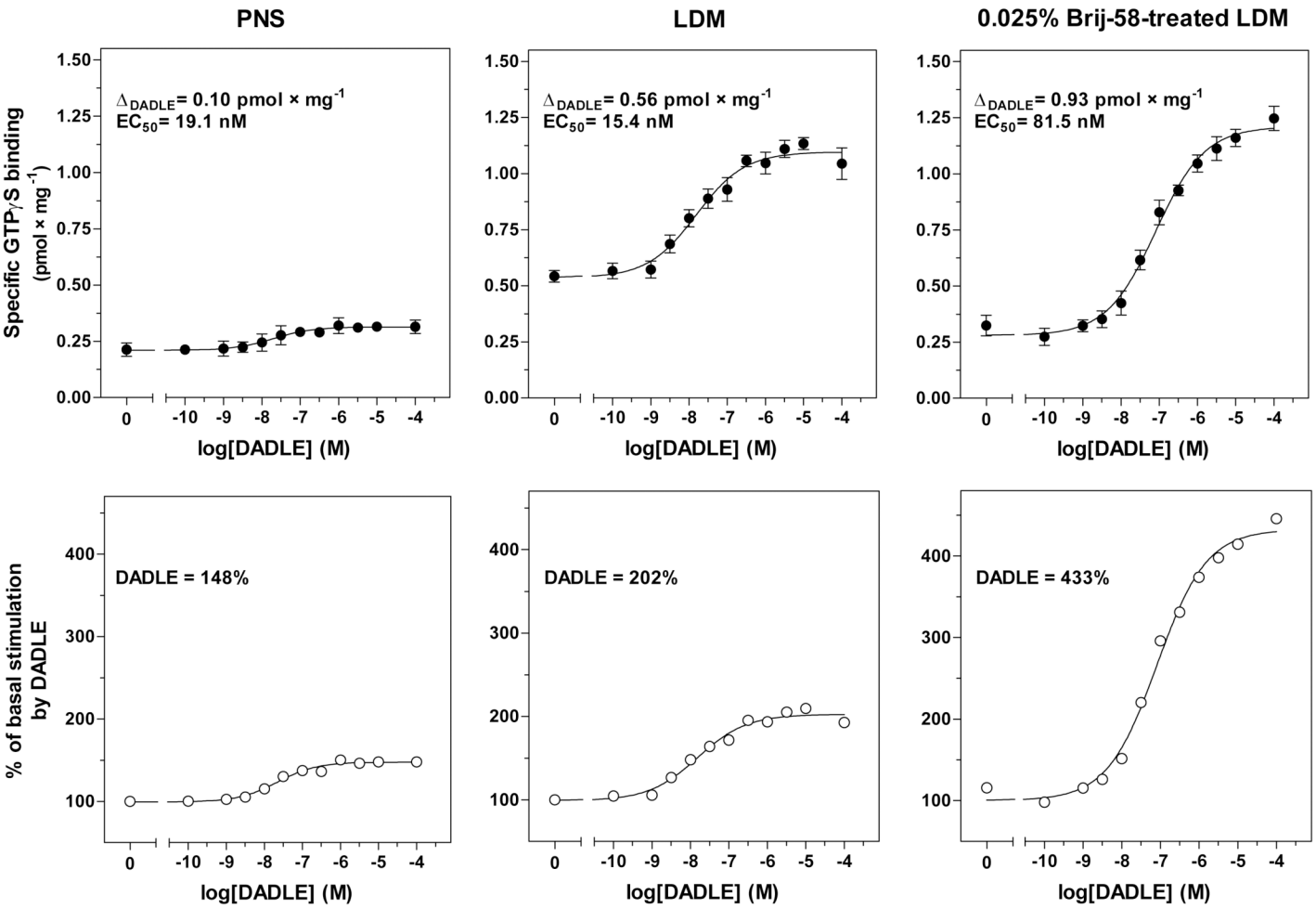

Fig 5. Dose-response curves of DADLE-stimulated [^{35}S]GTPγS binding; comparison of PNS, LDM and 0.025% Brij-58-treated LDM. Upper panels. Dose-response curves of DADLE-stimulated [^{35}S]GTPγS binding were measured in PNS, LDM and 0.025% Brij-58-treated LDM as described in Methods. LDM and 0.025% Brij-58-treated LDM represent the mixed pool of membranes in combined fractions 1–6 prepared from δ-OR-G_i1α cells in the absence or presence of detergent, respectively. The net increment of agonist-stimulation (Δ_{DADLE}) and DADLE concentration inducing the half-maximum response [EC_{50} (DADLE)] were determined by GraphPad Prism4. **Lower panels.** The ratio between the agonist-stimulated (DADLE) and the basal level of [^{35}S]GTPγS binding was expressed as % of agonist stimulation over the basal level; the basal level represented 100%. Results represent the average of 3 experiments ± SEM. The significance of difference of EC_{50} and Δ_{DADLE} in PNS versus LDM versus 0.025% Brij-58-treated LDM was determined by one-way ANOVA followed by Bonferroni´s multiple comparison test using GraphPad Prism4 (see S5 Table).

doi:10.1371/journal.pone.0135664.g005

stimulation (Δ_{DADLE}) in fractions 5+6 was increased by Brij-58 from 0.19 ± 0.02 to 0.26 ± 0.02 pmol × mg^{-1}. In fraction 4, Δ_{DADLE} was increased from 0.07 ± 0.01 to 0.28± 0.02 pmol × mg^{-1} (Fig 8). The average net increment of agonist stimulation in combined fractions 4+5+6 was 1.8-fold higher than in the same fractions prepared in the absence of detergent.

In this set of experiments, we have also determined theδ-OR number by agonist binding assay using[^{3}H]DADLE. As expected from the previous results of antagonist binding (Fig 7), the level of specific [^{3}H]DADLE binding in 0.025% Brij-58-treated fractions 5–6 was ≈2-fold lower than in the same fractions prepared in the absence of detergent (Fig 9). The detergent-induced shift of receptors to lower densities was noticed as an increase of [^{3}H]DADLE binding in fraction 4 from 0.60 ± 0.02 to 1.21 ± 0.03 pmol × mg^{-1} proceeding in parallel with the decrease of agonist binding in fractions 5–6 from 1.86 ± 0.03 to 1.00 ± 0.03 pmol × mg^{-1}. The sum of [^{3}H]DADLE binding in fractions 4, 5 and 6 was decreased by Brij-58 from 4.32 ± 0.04

Table 3. DADLE- stimulated [^{35}S]GTPγS binding in membranes prepared from PTX-untreated cells; dose-response curves.

	PNS	LDM	0.025% Brij-58-treated LDM
Δ_{DADLE}	0.10	0.56**	0.93***
Δ_{DADLE}/B_{max}	0.18	0.16ND	0.53**
EC_{50}	19.1	15.4ND	81.5**

Δ_{DADLE} (pmol × mg^{-1}), net increment of agonist stimulation at saturating concentration of DADLE; Δ_{DADLE}/B_{max} ratio, Δ_{DADLE} normalized to receptor number; EC_{50} (nM), DADLE concentration inducing half-maximum stimulation of [^{35}S]GTPγS binding.

* ($p<0.05$)

** ($p<0.01$)

*** ($p<0.001$) indicates a significant difference between PNS and LDM or 0.025% Brij-58-treated LDM; ND ($p>0.05$), not different.

doi:10.1371/journal.pone.0135664.t003

pmol × mg^{-1} to 3.21 ± 0.04 pmol × mg^{-1}. Normalization of the net increment of DADLE stimulation (Δ_{DADLE}) to δ-OR number (B) in fractions 4–6, indicated the 2.4-fold higher Δ_{DADLE}/B ratio in Brij-58-treated fractions than in the same fractions prepared in the absence of detergent (Table 5).

To obtain sufficient amount of protein for performance of a multiple assays, fractions 1–6 were combined together and used for determination of dose-response curves of DADLE-stimulated [^{35}S]GTPγS binding (Fig 10) and saturation binding assays of δ-OR by [^{3}H]DADLE (Fig 11). Comparison of the dose-response curves indicated that the potency of agonist response in 0.025% Brij-58-treated LDM (EC_{50} = 280 ± 15 nM) was significantly lower by one-order of magnitude than in LDM prepared in the absence of detergent (EC_{50} = 28 ± 4 nM) (Fig 10A, S10 Table). Contrarily, the % of agonist stimulation over the basal level in 0.025% Brij-58-treated LDM (372%) was higher than in LDM (283%) (Fig 10B).

Saturation of [^{3}H]DADLE binding sites in combined fractions 1–6 indicated the significant decrease of both affinity and maximum number of δ-OR in 0.025% Brij-58-treated LDM (K_d = 7.4 ± 2.2 nM; B_{max} = 0.6 ± 0.1 pmol × mg^{-1}) when compared with LDM prepared in the absence of detergent (K_d = 1.7 ± 0.7 nM; B_{max} = 1.1 ± 0.1 pmol × mg^{-1}) (Fig 11, S11 Table).

Thus, determination of functional response of G proteins to agonist stimulation in membranes prepared from PTX-treated δ-OR-$G_i1\alpha$ ($C^{351}I$)-HEK293 cells and normalization of this response to δ-OR number determined by agonist binding assay confirmed our previous results obtained in analysis of membranes prepared from PTX-untreated δ-OR-$G_i1\alpha$ ($C^{351}I$)-HEK293 cells.

Direct effect of Brij-58 on δ-OR-G protein coupling in isolated plasma membranes at 30°C

As noticed before in studies of baclofen-stimulated [^{35}S]GTPγS binding in Percoll-purified PM prepared from rat brain cortex [29], the non-ionic detergents Brij-58, Triton X-100 and digitonin were able, within the narrow range of detergent concentrations, to increase $GABA_B$-R agonist-stimulated [^{35}S]GTPγS binding when added directly to the assay medium. Exposure to higher detergent concentrations resulted in drop of G protein activity to zero level. In the case of Brij-58, this range was between 0.006 and 0.013% (w/v). Similar result was observed in PM isolated from δ-OR-$G_i1\alpha$ ($C^{351}I$)-HEK293 cells: the increase of DADLE-stimulated [^{35}S]GTPγS binding was detected at 0.006% Brij-58 (Fig 12). Importantly, activation of G proteins at this detergent concentration was detected in PM isolated from both PTX-untreated and

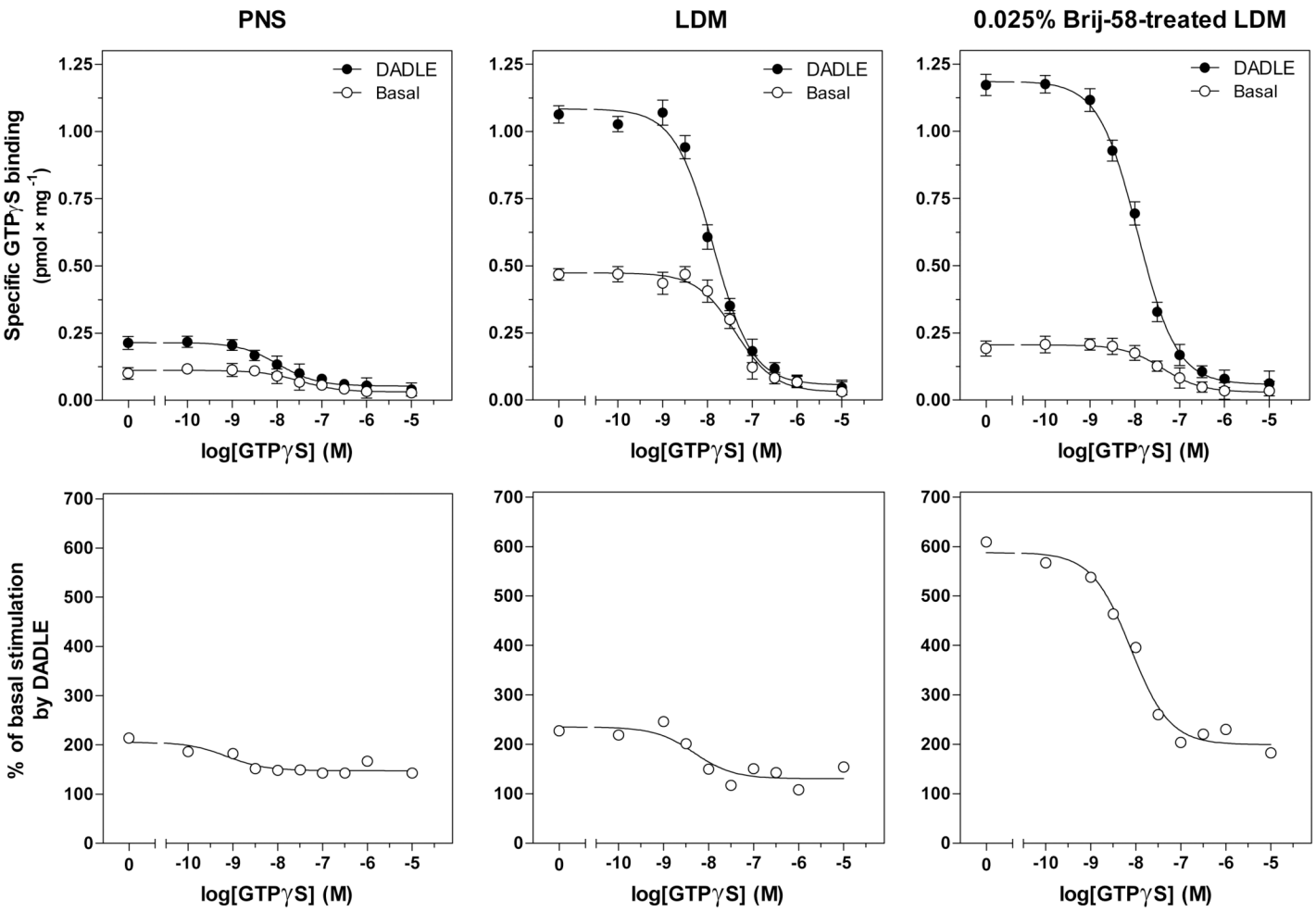

Fig 6. Competitive [^{35}S]GTPγS/GTPγS binding curves; comparison of PNS, LDM and 0.025% Brij-58-treated LDM. Upper panels. [^{35}S]GTPγS binding to PNS, LDM and 0.025% Brij-58-treated LDM prepared from δ-OR-G_i1α cells was measured in absence (B_0) or presence of increasing concentrations of unlabeled GTPγS as described in Methods; IC_{50} values were calculated by GraphPad Prism4. **Lower panels.** The ratio between the agonist-stimulated (DADLE) and the basal level of [^{35}S]GTPγS binding was expressed as % of agonist stimulation over the basal level; the basal level represented 100%. The data represent the average of 3 experiments ± SEM. The significance of difference of IC_{50} and ΔB_0 values in PNS versus LDM versus 0.025% Brij-58-treated LDM was determined one-way ANOVA followed by Bonferroni´s multiple comparison test using GraphPad Prism4 (see S6 Table).

doi:10.1371/journal.pone.0135664.g006

PTX-treated δ-OR-G_i1α cells (compare upper and lower panels in Fig 12). Therefore, the effect of Brij-58 on [^{35}S]GTPγS binding was manifested for G_i1α present within δ-OR-G_i1α ($C^{351}I$) fusion protein as well as for PTX-sensitive G proteins endogenously expressed in HEK293 cells.

In accordance with the data obtained in analysis of LDM isolated at 0°C, comparison of the dose-response curves of DADLE-stimulated [^{35}S]GTPγS binding in plasma membranes exposed to 0.006% Brij-58 at 30°C indicated a highly significant decrease in potency of agonist response: EC_{50} value was increased from 24 ± 5 nM (no detergent) to 120 ± 10 nM in PM exposed to 0.006% Brij-58 (Fig 13, S13 Table). The agonist binding to δ-OR was not affected at this detergent concentration (Fig 14A, S14 Table) and 0.02% concentration of Brij-58 was needed to achieve the half-maximum inhibition of [^{3}H]DADLE binding (Fig 14B). It should be noticed that at this detergent concentration, DADLE-stimulated [^{35}S]GTPγS binding was completely diminished (Fig 12). Therefore, agonist binding to δ-OR was substantially less

Table 4. DADLE-stimulated [^{35}S]GTPγS binding in membranes prepared from PTX-untreated cells; [^{35}S]GTPγS/GTPγS competition binding curves.

		PNS	LDM	0.025% Brij-58-treated LDM
(-DADLE)				
	B_0	0.11	0.47**	0.21*
	B_0 (-DADLE)/B_{max}	0.20	0.13ND	0.12ND
	IC_{50}	32.7	42.3ND	41.9ND
(+DADLE)				
	B_0	0.22	1.08**	1.19**
	B_0 (+DADLE)/B_{max}	0.39	0.30ND	0.68*
	IC_{50}	10.6	13.5ND	11.6ND
ΔB_0		0.11	0.61**	0.98***
$\Delta B_0/B_{max}$		0.20	0.17ND	0.56*

B_0 (pmol × mg^{-1}), [^{35}S]GTPγS binding in the absence of GTPγS; ΔB_0, the difference between B_0 (+DADLE) and B_0 (-DADLE); $\Delta B_0/B_{max}$ ratio, ΔB_0 normalized to receptor number; IC_{50} (nM), GTPγS concentration inducing half-maximum inhibition of [^{35}S]GTPγS binding.

* ($p<0.05$)

** ($p<0.01$)

*** ($p<0.001$) indicates a significant difference between PNS and LDM or 0.025% Brij-58-treated LDM; ND ($p>0.05$), not different.

doi:10.1371/journal.pone.0135664.t004

sensitive to deteriorating effect of detergent than receptor ability to activate G proteins. This conclusion was in our experiments demonstrated for PTX-insensitive $G_i1\alpha$ ($C^{351}I$) covalently bound to δ-OR as well as for PTX-sensitive G proteins endogenously expressed in HEK293 cells.

The effect of Brij-58 on hydrophobic plasma membrane interior

Measurement of steady-state anisotropy of hydrophobic membrane probe DPH indicated that Brij-58 exhibited a strong "fluidization" of hydrophobic plasma membrane interior (Fig 15). When increasing Brij-58 above the critical micelle concentration (CMC = 0.0086% w/v), the highly polarized signal of DPH observed in detergent-untreated PM ($r_{DPH} = 0.224 \pm 0.003$) was gradually decreased to the highly depolarized signal at high detergent concentrations ($r_{DPH} = 0.087 \pm 0.003$), which was close to that of Brij-58 alone in aqueous medium at 25°C ($r_{DPH} = 0.072 \pm 0.001$).

More detailed understanding of the detergent effect on organization of PM microenvironment was obtained by determination of the lifetime values of DPH fluorescence and analysis of the time-resolved DPH anisotropy decay by "wobble in cone" model [30,31]. As shown in Table 6, the average lifetime of DPH fluorescence (τ_{av}) was continuously decreased by increasing detergent concentrations. The S-order parameter decreased as well and this decrease proceeded in parallel with the increase of wobbling diffusion constant D_w (Fig 16). Accordingly, the values of rotational correlation time (ϕ) were decreased. Thus, the lower friction of DPH molecules within plasma membrane microenvironment and higher rate of DPH rotation was detected.

Discussion

According to the collision-coupling model of receptor-G protein interaction [32], the level of G protein activated is independent of the concentration of agonist-bound receptors, but the rate of G protein activation is proportional to the concentration of agonist-bound receptors. Thus, reduction of receptor density should cause no reduction in the maximal level of G protein

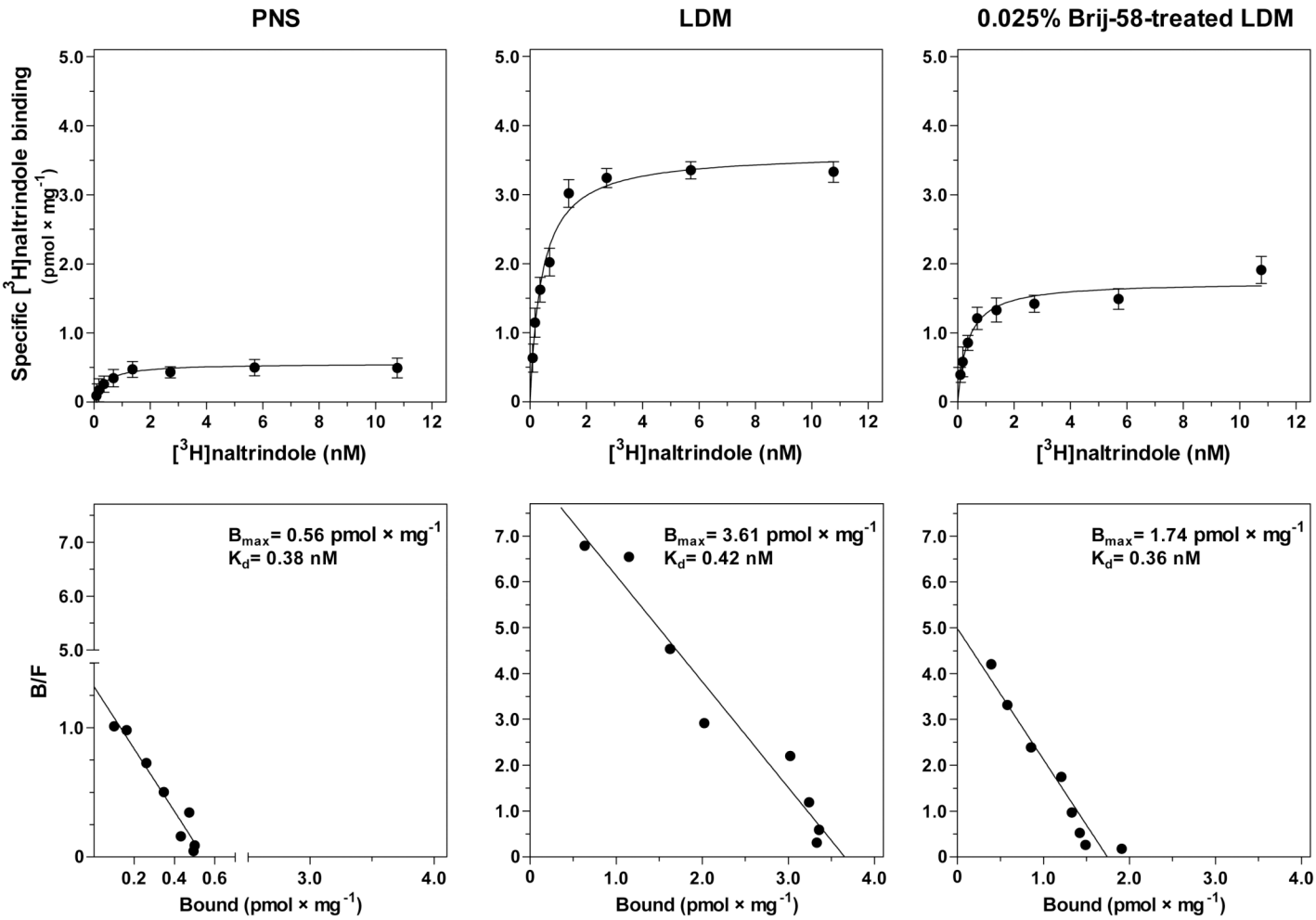

Fig 7. Saturation of [^{3}H]naltrindole binding sites in PNS, LDM and 0.025% Brij-58-treated LDM. Saturation binding studies of specific δ-opioid antagonist [^{3}H]naltrindole sites in PNS, LDM and 0.025% Brij-58-treated LDM was measured as described in Methods. The B_{max} and K_d values were calculated by GraphPadPrism4. The data represent the average of 3 experiments ± SEM. Significance of difference of B_{max} and K_d values in PNS versus LDM versus 0.025% Brij-58-treated LDM was determined one-way ANOVA followed by Bonferroni´s multiple comparison test using GraphPad Prism4 (see S7 Table).

doi:10.1371/journal.pone.0135664.g007

activation but it should reduce the rate of G protein activation and decrease the EC_{50} values of agonist-stimulated G protein activity. It was also suggested that diffusion of receptors and effectors is slow, so that receptors will only activate effectors that are in their vicinity at the time of agonist occupation [33,34]. The rate of G protein activation was found to be dependent on the agonist binding frequency relative to the encounter time of G protein and receptor [35,36].

The test of validity of collision-coupling model for opioid receptors was performed in C6 cells expressing different amounts of μ- and δ-OR and G proteins [37]. The time-course of full or partial agonist-stimulated [^{35}S]GTPγS binding did not vary in cells containing widely different amounts of μ-OR or δ-OR and the 10-fold reduction of the functional complement of G proteins by pertussis toxin caused the decrease of maximum agonist-stimulated [^{35}S]GTPγS binding. The association rate of [^{35}S]GTPγS with agonist-activated G protein was unchanged. Results of this study were not compatible with the random collision-coupling model but

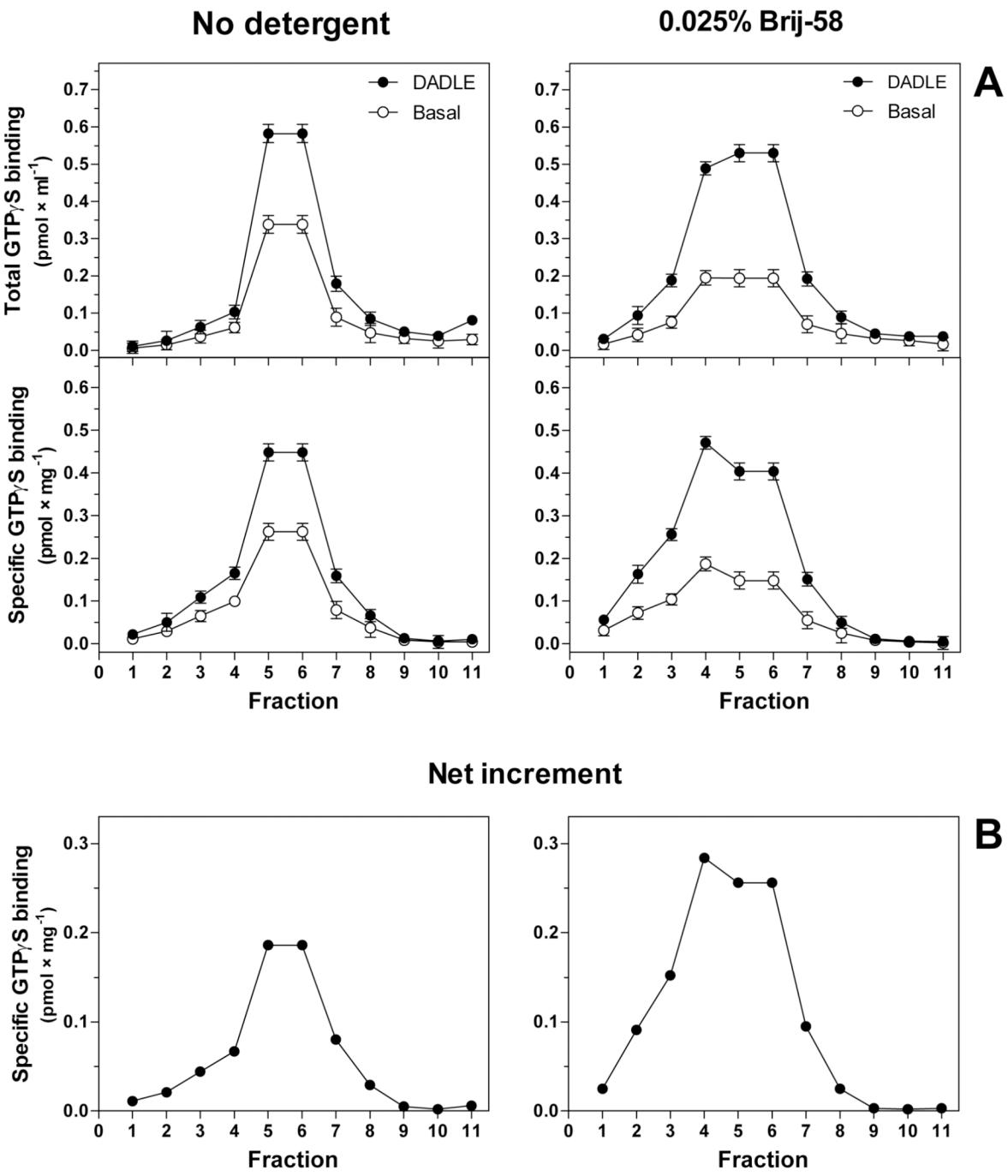

Fig 8. Subcellular fractionation of PTX-treated δ-OR-$G_i1α$ cells; density gradient profiles of basal and DADLE-stimulated [^{35}S]GTPγS binding. Pertussis toxin-treated δ-OR-$G_i1α$ cells were homogenized and fractionated in the absence (no detergent) or presence of 0.025% Brij-58 in sucrose gradient as in studies of PTX-untreated cells (see Methods). (**A**) Basal (○) and DADLE-stimulated (●) [^{35}S]GTPγS binding was measured in fractions collected from the top to bottom of the centrifuge tube and expressed as total (pmol × ml^{-1}) or specific binding (pmol × mg^{-1}) in a given fraction. (**B**) Net increment of DADLE stimulation ($Δ_{DADLE}$) was calculated as the difference between specific DADLE-stimulated and basal level of [^{35}S]GTPγS binding and expressed as pmol × mg^{-1}. Results represent the average of 3 experiments ± SEM. The significance of difference between the specific DADLE-stimulated and basal [^{35}S] GTPγS binding in fractions was determined by Student´s t-test (see S8 Table).

doi:10.1371/journal.pone.0135664.g008

supported a compartmentalization model [38–40] in which receptors and G proteins are "in some way" associated together and compartmentalized within plasma membrane.

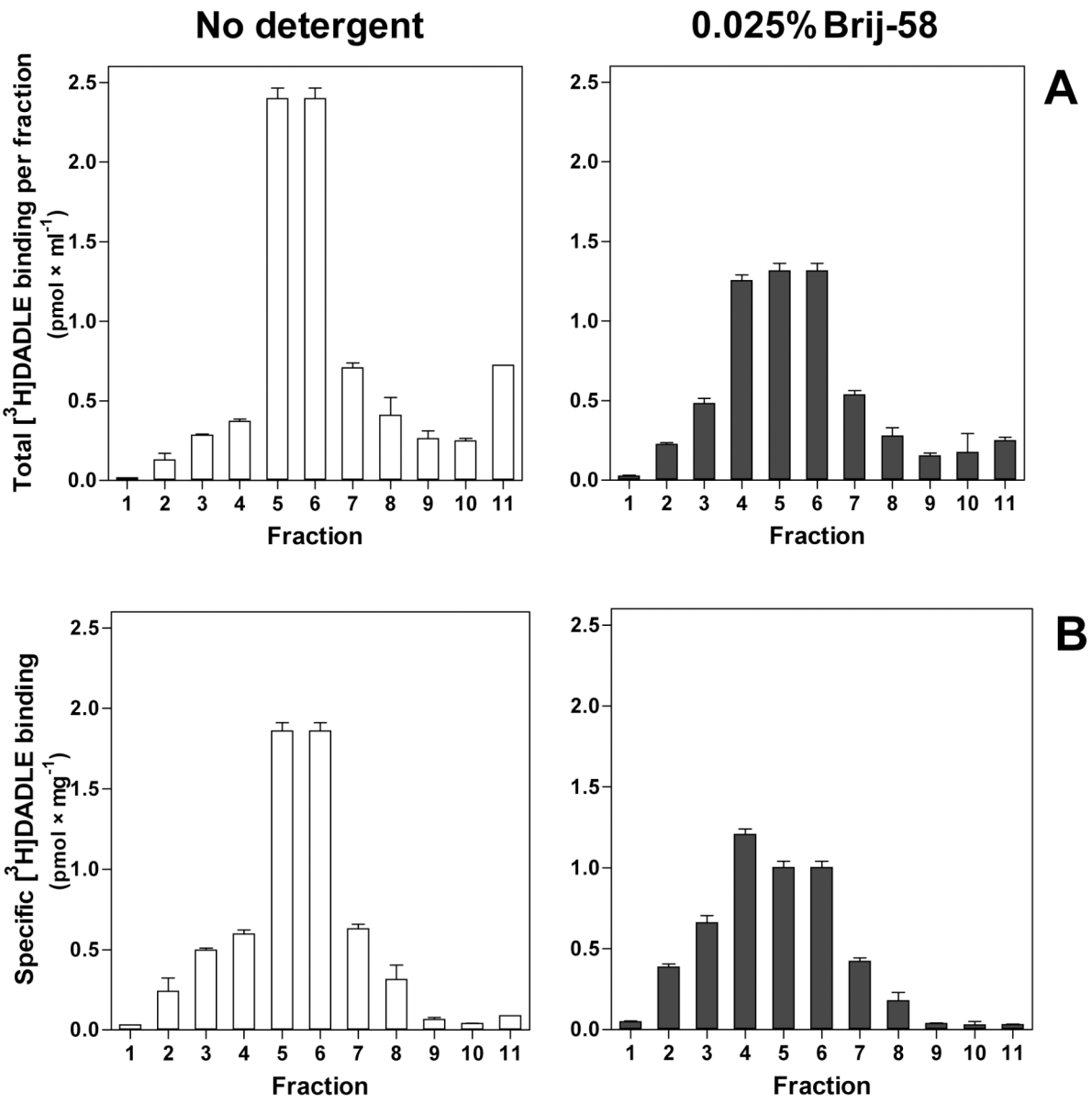

Fig 9. Density gradient profiles of [^{3}H]DADLE binding; PTX-treated δ-OR-G$_i$1α cells. PTX-treated δ-OR-G$_i$1α cells were homogenized and fractionated as described in legend to Fig 8. **(A)** [^{3}H]DADLE binding was determined in fractions as described in Methods and expressed as total binding (pmol × ml^{-1}) or **(B)** specific binding (pmol × mg^{-1}) in a given fraction at the saturating 10 nM concentration. Results represent the average of 3 experiments ± SEM. The significance of difference of [^{3}H]DADLE binding between fractions collected from gradients containing no detergent and 0.025% Brij-58 was determined by Student´s t-test (see S9 Table).

doi:10.1371/journal.pone.0135664.g009

The association of GPCRs and G proteins with the plasma membrane makes them susceptible to their lipid environment so that lipid-protein interactions are important for their function [41]. In direct relevance to theoretical models of receptor-G protein coupling, plasma membrane domains/rafts were suggested as devices concentrating the signaling molecules, i.e. bringing them into a closer spatial organization than just the random order arrangement within the fluid mosaic of proteins and lipids in the bulk of plasma membranes [1–6,9–12,16]. The content of trimeric G proteins and GPCR in these PM compartments responded dramatically to agonist stimulation [22,23,42–59].

Table 5. Net increment of DADLE-stimulated [^{35}S]GTPγS binding and [^{3}H]DADLE binding in sucrose fractions collected from PTX-treated δ-OR-G$_i$1α cells.

	No detergent		0.025% Brij-58	
Fraction	**4**	**5+6**	**4**	**5+6**
Δ_{DADLE}	0.07	0.19	0.28**	0.26*
B	0.60	1.86	1.21*	1.00*
Δ_{DADLE}/B	0.11	0.10	0.23	0.26

Δ_{DADLE} (pmol × mg^{-1}), net increment of agonist stimulated [^{35}S]GTPγS binding at 10 μM DADLE; B (pmol × mg^{-1}), [^{3}H]DADLE binding at saturating 10 nM concentration; Δ_{DADLE}/B, ratio between Δ_{DADLE} and B.

* ($p<0.05$)

** ($p<0.01$) indicates a significant difference between the two types of membranes; ND ($p>0.05$), not different.

doi:10.1371/journal.pone.0135664.t005

More specifically, κ-OR were found to be localized in lipid rafts [60] and analysis of μ-OR- and δ-OR-G protein coupling indicated the compartmentalization of these signaling molecules in PM [37]. Cholesterol reduction by methyl-β-cyclodextrin was found to attenuate δ-OR-initiated signaling in neuronal cells but enhance it in non-neuronal cells [57]. In HEK293 cells stably expressing δ-OR-G$_i$1α fusion protein, cholesterol depletion by β-cyclodextrin resulted in decrease of potency of G protein response to agonist DADLE stimulation, but the maximum response was unchanged [26]. Adenylyl cyclase super-activation induced by prolonged exposure to morphine was found to be dependent on receptor localized within lipid rafts and independent of receptor internalization [61]. Palmitoylation and membrane cholesterol stabilized the homo-oligomerization of μ-OR and coupling with G proteins [62].

Furthermore, experiments based on plasmon-waveguide resonance spectroscopy [63] indicated that the unbound, inactive δ-OR receptors were enriched in 1, 2-palmitoyl-oleoyl-sn-glycero-3-phosphoserine (POPC)-rich domain of lipid bilayer composed of 1:1 mixture of POPC and sphingomyelin (SM). The agonist- and antagonist-bound receptors were concentrated in SM-rich component (with a two-fold greater propensity in the case of the agonist) characterized by a greater thickness. Since it is known that receptor activation involves changes in the orientation of trans-membrane helices with an increase in receptor vertical length, i.e. perpendicular to the plane of the plasma membrane [64], it was hypothesized that the driving force for receptor redistribution comes from the increased hydrophobic match of the elongated receptor for the thicker SM-enriched part of the bilayer, a sorting mechanism that has previously been observed in other subcellular compartments [65,66].

Literature data mentioned above justify the effort to analyze in details the interaction of detergents with various plasma membrane preparations containing the functional GPCR and G proteins with the aim to find "some correlation" between the structural and dynamic state of the membrane lipid bilayer and parameters of GPCR-G protein coupling. Obviously, this type of analysis requires the step by step determination of concentration dependency of detergent effect.

Comparison of LDM isolated from PTX-untreated and PTX-treated δ-OR-G$_i$1α (C^{351}I)-HEK293 cells in the absence or presence of low concentrations of Brij-58 at 0°C indicated the decrease of δ-OR number in Brij-58-treated LDM when compared with detergent-untreated LDM (**Figs** 7 and 9). The decrease of δ-OR was measured by both agonist and antagonist binding assays and accompanied by a decrease in potency of agonist response (**Figs** 4, 5 and 10). This was demonstrated by comparison of the dose-response curves of both DADLE-stimulated

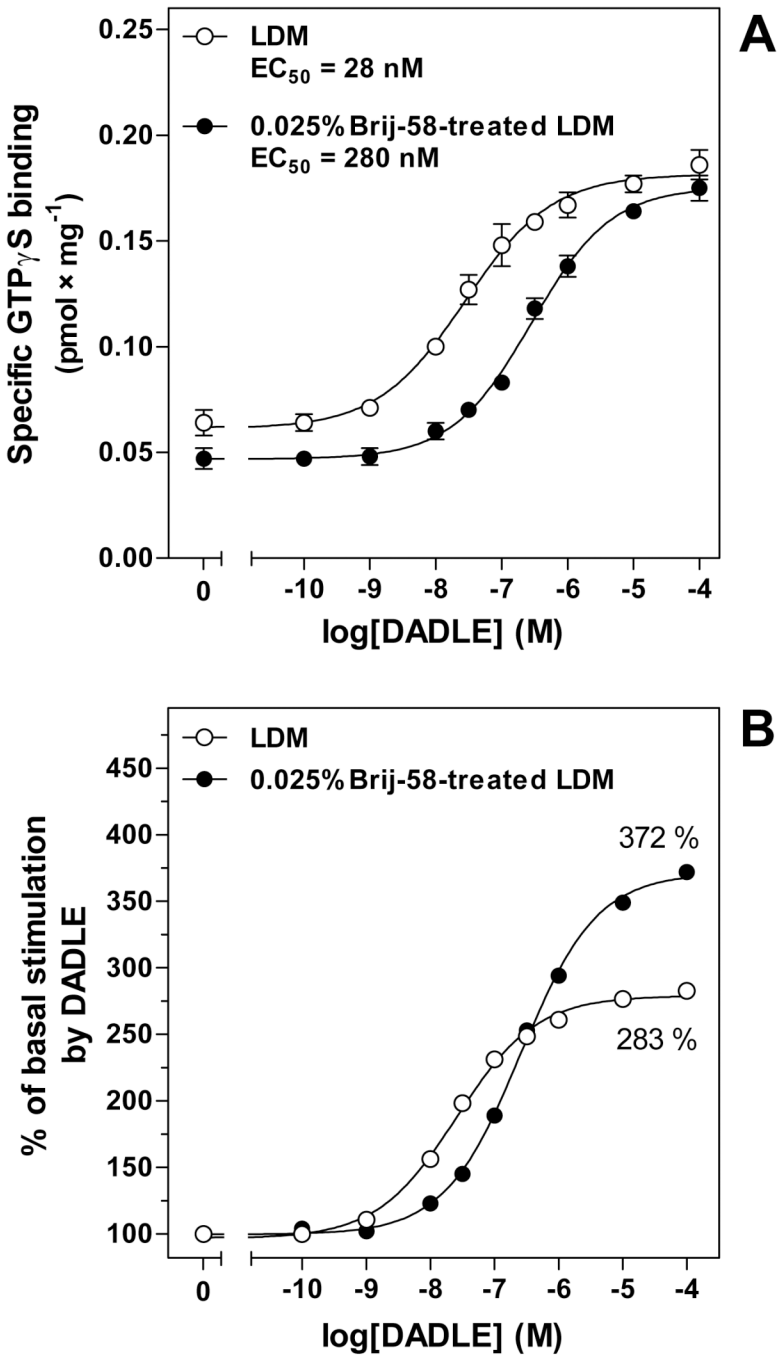

Fig 10. Dose-response curves of DADLE-stimulated [^{35}S]GTPγS binding in LDM and 0.025% Brij-58-treated LDM prepared from PTX-treated δ-OR-G$_i$1α cells. Sucrose gradient fractions 1–6 were combined together, mixed and used for determination of the dose-response curves of DADLE-stimulated [^{35}S]GTPγS binding as described in Methods. **(A)**. DADLE concentration inducing the half-maximum response [EC_{50} (DADLE)] was determined by GraphPad Prism4. **(B)** The ratio between the DADLE-stimulated and basal level of [^{35}S]GTPγS binding was expressed as % of agonist stimulation over the basal level; the basal level represented 100%. Results represent the average of 3 experiments ± SEM. LDM, fractions collected from gradient containing no detergent; 0.025% Brij-58-treated LDM, fractions collected from gradient containing 0.025% Brij-58.

doi:10.1371/journal.pone.0135664.g010

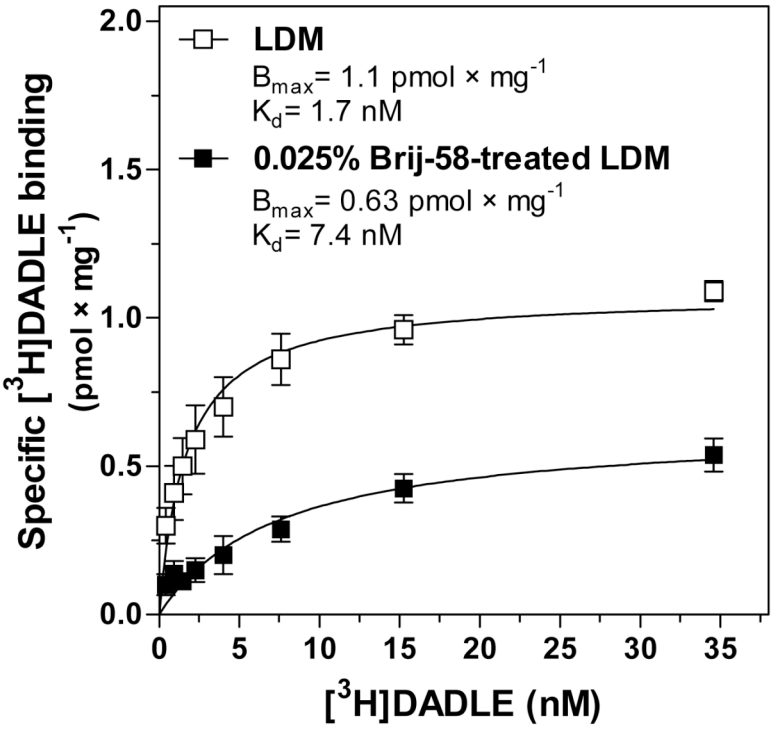

Fig 11. Saturation of [^{3}H]DADLE binding sites in LDM and 0.025% Brij-58-treated LDM prepared from PTX-treated δ-OR-G$_i$1α cells. Saturation of specific [^{3}H]DADLE binding sites was measured as described in Methods. The B_{max} and K_d values were calculated by GraphPadPrism4. The data represent the average of 3 experiments ± SEM. LDM, fractions collected from gradient containing no detergent; 0.025% Brij-58-treated LDM, fractions collected from gradient containing 0.025% Brij-58

doi:10.1371/journal.pone.0135664.g011

[^{32}P]GTPase (Fig 4) and [^{35}S]GTPγS binding (**Figs** 5 and 10). However, the maximum G protein response (efficacy) was significantly increased (**Tables** 1–5). Similar data were obtained in analysis of the direct effect of increasing concentrations of Brij-58 on isolated plasma membranes at 30°C (**Figs** 12–14).

When interpreting these results, it is logical to assume that the increase of detergent concentration at hydrophobic interface of δ-OR (exposed to the bulk lipid phase of the membrane) removes lipids attached to the outer surface of protein molecule (lipid annulus) and in this way perturbs the optimum lipid environment of δ-OR needed for its optimum function. This is reflected first as a transitional increase of efficacy of G protein response to agonist stimulation accompanied by decrease of potency. Subsequently, at high detergent concentration, receptor is unable to find the proper, agonist-responding conformation and G protein response in completely diminished.

It may be also visualized that limited degradation of organized PM structure by detergent in critical range of low concentrations (0.01–0.1% Brij-58 at 0°C) might detach G proteins from the inhibitory effect of caveolin [15,50,67,68] or that the detergent-induced change of structural organization of lipid annulus surrounding δ-OR alters the oligomerization state of OR and, consequently, parameters of functional coupling between OR and their cognate G proteins [69–77].

Our previous results [29] indicated that DPH anisotropy (r_{DPH}) represents a useful parameter for analysis of detergent effect on membranes isolated from brain. In δ-OR-G$_i$1α (C^{351}I)-HEK293 cells, the decrease of r_{DPH} by Brij-58 (Fig 15) was 5-fold higher than that induced by

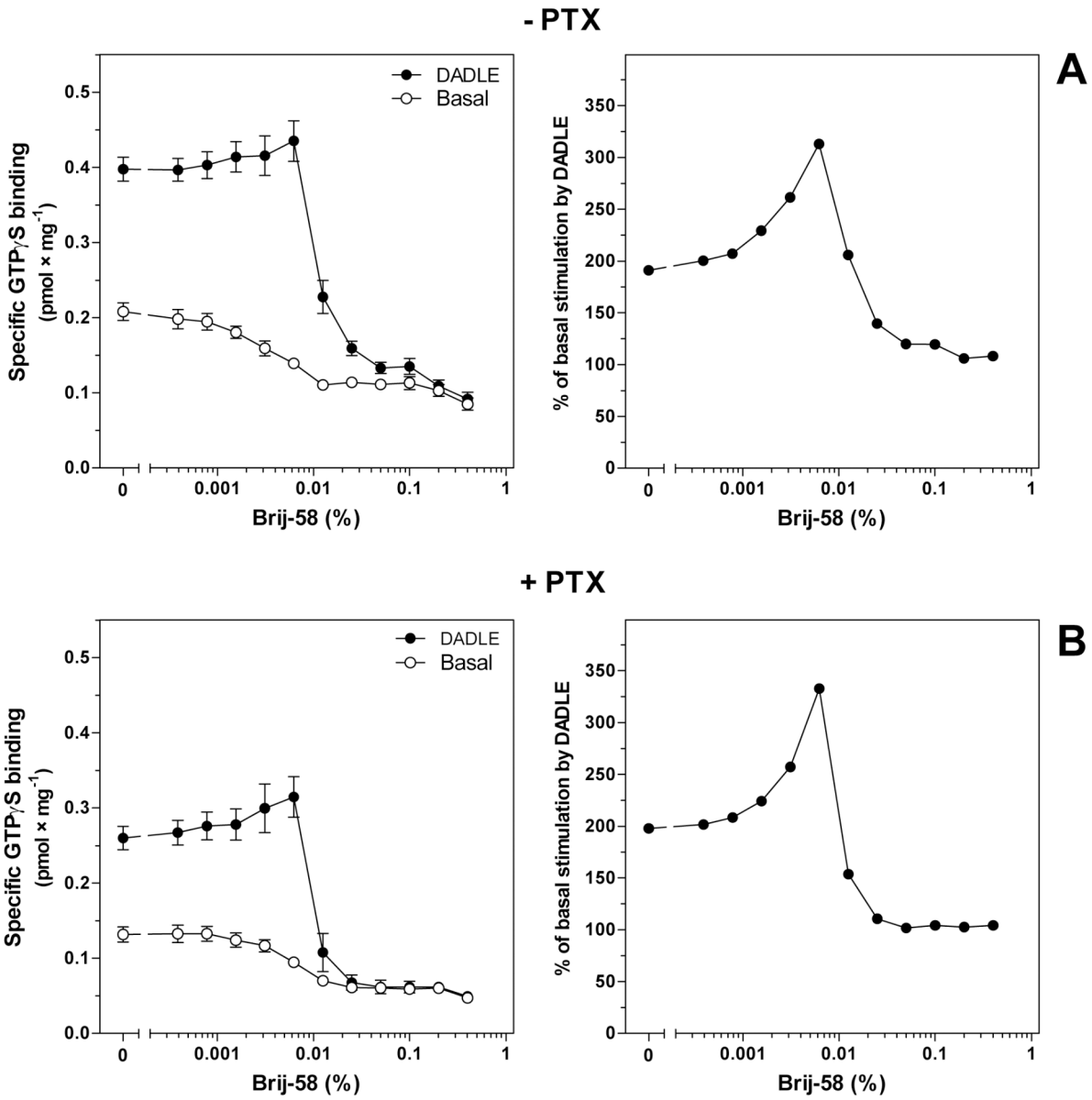

Fig 12. Direct effect of increasing concentrations of Brij-58 on basal and DADLE-stimulated [^{35}S]GTPγS binding at 30°C; PM isolated from PTX-treated and untreated δ-OR-G$_i$1α cells. Basal and DADLE-stimulated [^{35}S]GTPγS binding was measured in Percoll-purified plasma membranes isolated from (**A**) PTX-untreated (-PTX) and (**B**) PTX-treated (+PTX) δ-OR-G$_i$1α (C^{351}I)-HEK293 cells. Increasing concentrations of Brij-58 were added directly into the assay medium and incubated for 30 min at 30°C. The data represent the average of 3 experiments ± SEM. Significance of difference between the specific DADLE-stimulated and basal [^{35}S]GTPγS binding was determined by Student´s t-test (see S12 Table).

doi:10.1371/journal.pone.0135664.g012

cholesterol depletion [26]. The highly polarized signal of DPH, measured in PM in absence of detergent (r_{DPH} = 0.224), was decreased to the highly depolarized signal (r_{DPH} = 0.087) detected at high detergent concentrations. The application of "wobble in cone" model enabled us to retrieve the information about membrane dynamics characterized by wobbling diffusion constant (D_w). This model also enabled us to gain the "static" information about the degree of the orientation constrains of rotational movements of DPH dye by calculation of S-order parameter (S). The time-resolved analysis of DPH fluorescence by the "wobble in cone model" of DPH motion (**Table 6** and **Fig 16**) indicated that the exposure of PM to the increasing

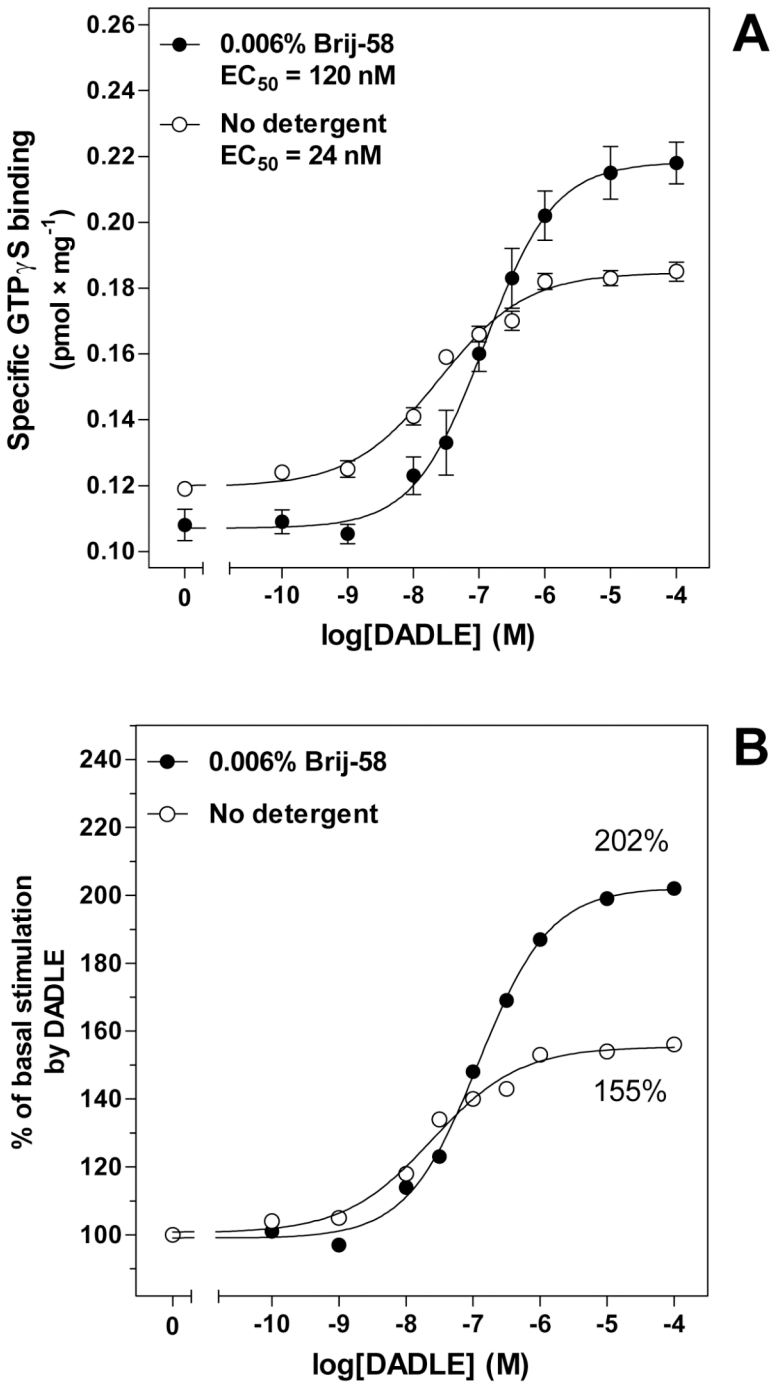

Fig 13. Dose-response curves of DADLE-stimulated [^{35}S]GTPγS binding in PM isolated from δ-OR-G$_i$1α cells; direct effect of 0.006% Brij-58 at 30°C. (**A**) Dose-response curves of DADLE-stimulated [^{35}S]GTPγS binding were measured in plasma membranes isolated from δ-OR-G$_i$1α (C^{351}I)-HEK293 cells in the absence (○) or presence (●) of 0.006% Brij-58 as described in Methods in binding assay medium at 30°C. (**B**) The ratio between the DADLE-stimulated and the basal level of [^{35}S]GTPγS binding was expressed as % of agonist stimulation over the basal level; the basal level represented 100%. The data represent the average of 3 experiments ± S.E.M.

doi:10.1371/journal.pone.0135664.g013

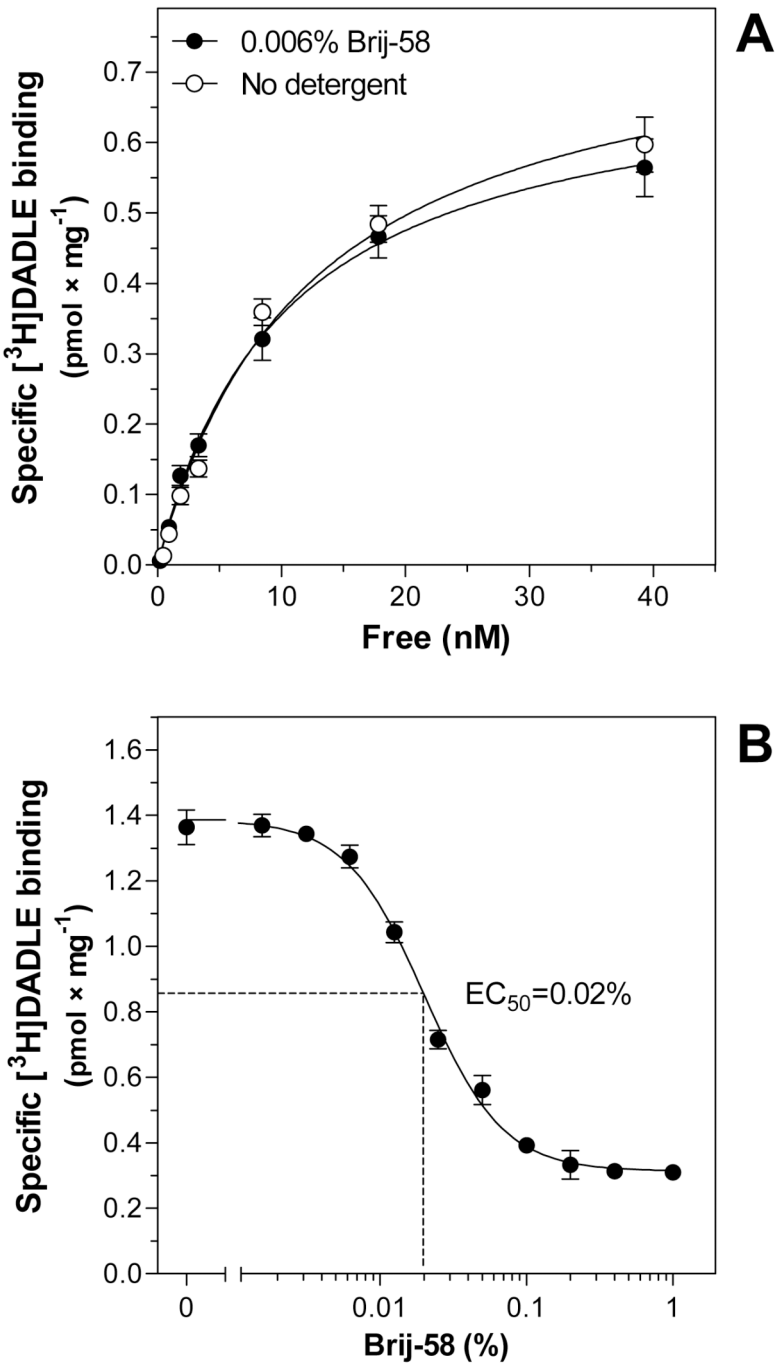

Fig 14. Saturation of [^{3}H]DADLE binding sites in PM isolated from δ-OR-G_i1α cells; direct effect of 0.006% Brij-58 at 30°C. (**A**) Saturation of δ-OR agonist [^{3}H]DADLE binding sites was measured in plasma membranes isolated from δ-OR-G_i1α (C^{351}I)-HEK293 cells as described in Methods in the absence (○) or presence (●) of 0.006% Brij-58 in binding assay medium at 30°C. The B_{max} and K_d values were calculated by GraphPad Prism4. (**B**) Effect of increasing concentrations of Brij-58 on [^{3}H]DADLE binding was measured in PM isolated in the absence of detergent; 50% inhibition of agonist binding was observed at 0.02% Brij-58. The data represent the average of 3 experiments ± S.E.M.

doi:10.1371/journal.pone.0135664.g014

concentrations of Brij-58 led to a higher motional freedom of the dye (increase of D_w) and a less structurally ordered structure of membrane bilayer (decrease of S-order parameter).

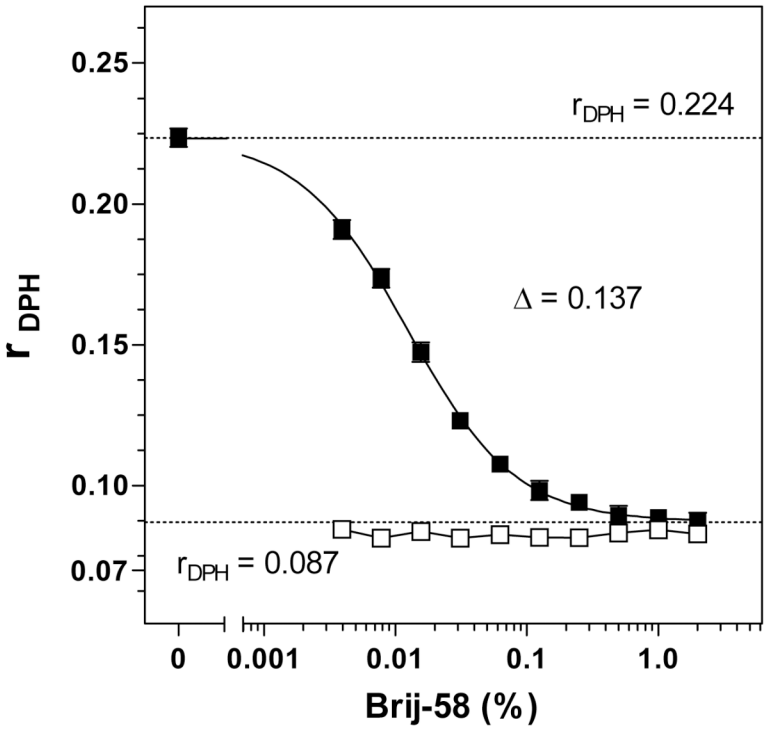

Fig 15. Effect of increasing concentrations of Brij-58 on „membrane fluidity"of isolated PM; steady-state anisotropy of fluorescence of diphenylhexatriene (r_{DPH}). Suspension of Percoll-purified PM in 50 mM Tris-HCl, pH 7.4 (0.2 mg protein per ml) was quickly mixed with 1 mM DPH in acetone (to 1 μM final concentration) and incubated under stirring for 60 min at 25°C.Anisotropy of DPH fluorescence (r_{DPH}) was measured at Ex 365/Em 425 nm wavelengths as described in Methods. (■), membranes plus Brij-58; (□), Brij-58 alone. The data shown represent the average of 3 experiments ± SEM.

doi:10.1371/journal.pone.0135664.g015

The existence of "critical range" of detergent concentrations inducing the limited membrane damage before the total collapse of plasma membrane structure and diminution of membrane protein function was also detected for $GABA_B$-receptors in plasma membranes isolated from rat forebrain cortex [29]. In close analogy to the data presented in this work (Fig 12), the clearly defined stimulatory [Brij-58, 0.006–0.013% w/v; Triton X-100, 0.013–0.025%) and

Table 6. The influence of increasing concentrations of Brij-58 on parameters of the time-resolved DPH fluorescence.

Brij-58 (%)	τ_1	τ_2	τ_{av}	r_0	r_∞	ϕ	S	D_w
0	2.68	9.70	8.35	0.26	0.136	5.59	0.73	0.020
0.0004	2.58	9.84	8.13	0.26	0.131	5.47	0.71	0.020
0.0016	2.29	9.50	7.68	0.27	0.103	4.26	0.62	0.033
0.0062	2.26	8.91	7.56	0.27	0.089	2.67	0.57	0.059
0.025	1.62	7.75	7.40	0.27	0.029	2.14	0.33	0.105
0.1	1.61	7.31	7.12	0.27	0.002	2.32	0.09	0.110

PM isolated from δ-OR-$G_i1\alpha$ ($C^{351}I$)-HEK293 cells were exposed to increasing concentrations of Brij-58 for 30 minutes at 25°C and labeled by DPH (1 μM, 30 min). Fluorescence lifetime and parameters of time-resolved decays of anisotropy of DPH fluorescence were determined as described in Methods. τ_1 and τ_2, the short- and long- components of lifetime of DPH fluorescence; τ_{av}, average lifetime; r_0, limiting anisotropy at time zero; r_∞, residual anisotropy; ϕ, rotational correlation time; S, S-order parameter; D_w, wobbling diffusion constant.

doi:10.1371/journal.pone.0135664.t006

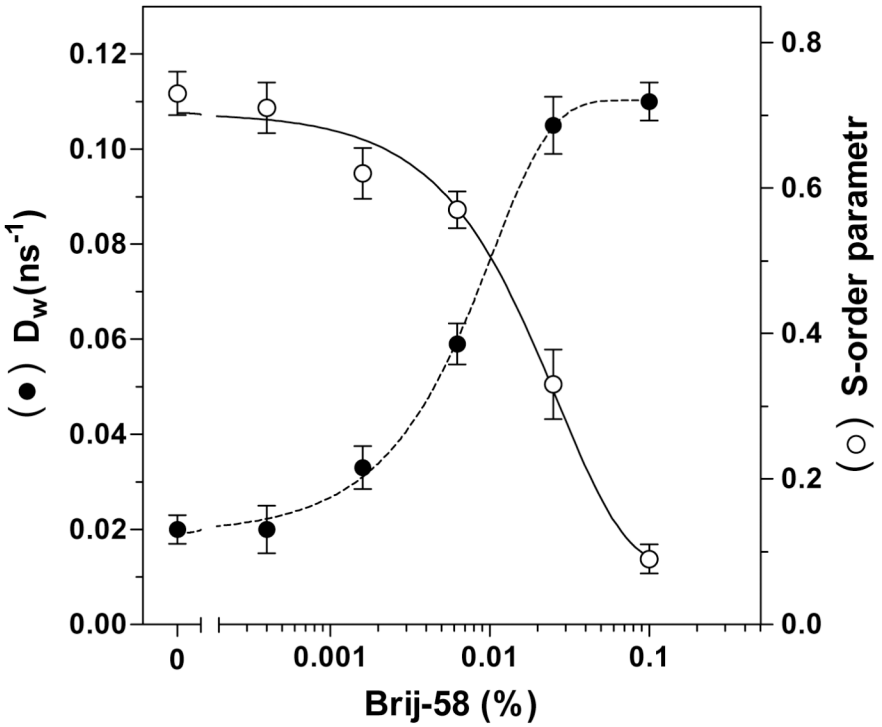

Fig 16. The effect of increasing concentrations of Brij-58 on time-resolved parameters of DPH fluorescence in PM; wobbling constant D_w and S-order parameter. The decay of anisotropy of DPH fluorescence in ns range was measured in PM isolated from PTX-untreated cells and analyzed as described in Methods. D_w, wobbling diffusion constant (●) and S-order parameter (○) were calculated according to the "wobble in cone" model of DPH mobility in membrane bilayer. The data shown represent the average of three experiments.

doi:10.1371/journal.pone.0135664.g016

inhibitory [Brij-58, >0.02% w/v; Triton X-100, >0.05% w/v) range of detergent concentrations was observed.

Conclusions

1) This work describes the simple method for preparation of intermediate forms of low-density, detergent-treated plasma membrane fragments (Brij-58-treated LDM) which are distinct from detergent-untreated PM fragments (LDM) exhibiting the same density but, on the other hand, do not represent the typical detergent-resistant membrane domains (DRMs) isolated in 0.5–1% Triton-X100 at 0°C. The "typical" DRMs contain less than 1% of original PM protein, large portion (30–40%) of trimeric G proteins, caveolin and flotilin but do not exhibit the functional coupling between δ-OR and G proteins due to deleterious effect of high detergent concentrations.

2) In optimum range of detergent concentrations (0.025–0.05% w/v), Brij-58-treated, low-density membranes exhibited 2-3-fold higher efficacy of DADLE-stimulated, high-affinity [γ-^{32}P]GTPase and [^{35}S]GTPγS binding than membranes of the same density prepared in the absence of detergent. The potency of agonist DADLE response was significantly decreased. At high detergent concentrations (>0.1%), the functional coupling between δ-OR and G proteins was completely diminished. The same detergent effects were measured in LDM isolated from PTX-treated cells. Therefore, the effect of Brij-58 on δ-OR-G protein coupling was not

restricted to the covalently bound $G_i1\alpha$ within δ-OR-$G_i1\alpha$ fusion protein, but it was also valid for PTX-sensitive G proteins of G_i/G_o family endogenously expressed in HEK293 cells.

Supporting Information

S1 Table. Statistical analysis of [^{32}P]GTPase activity in gradient fractions. Sucrose density gradients (1)-(4) were prepared from PTX-untreated δ-OR-$G_i1\alpha$ cells.
(DOCX)

S2 Table. Statistical analysis of [^{35}S]GTPγS binding in gradient fractions. Sucrose density gradients (1)-(3) were prepared from PTX-untreated δ-OR-$G_i1\alpha$ cells.
(DOCX)

S3 Table. Statistical analysis of [^{32}P]GTPase activity in PNS, LDM and 0.025% Brij-58-treated LDM.
(DOCX)

S4 Table. Statistical analysis of dose-response curves of DADLE-stimulated [^{32}P]GTPase activity. Comparison of PNS versus LDM and 0.025% Brij-58-treated LDM.
(DOCX)

S5 Table. Statistical analysis of dose-response curves of DADLE-stimulated [^{35}S]GTPγS binding. Comparison of PNS versus LDM and 0.025% Brij-58-treated LDM.
(DOCX)

S6 Table. Statistical analysis of competitive [^{35}S]GTPγS/GTPγS binding displacement curves. Comparison of PNS versus LDM and 0.025% Brij-58-treated LDM.
(DOCX)

S7 Table. Statistical analysis of [^{3}H]naltrindole saturation binding curves. Comparison of PNS versus LDM and 0.025% Brij-58-treated LDM.
(DOCX)

S8 Table. Statistical analysis of [^{35}S]GTPγS binding in gradient fractions. Sucrose density gradients were prepared from PTX-treated δ-OR-$G_i1\alpha$ cells in absence (no detergent) or presence of 0.025% Brij-58.
(DOCX)

S9 Table. Statistical analysis of [^{3}H]DADLE binding in gradient fractions. Sucrose density gradients were prepared from PTX-treated δ-OR-$G_i1\alpha$ cells.
(DOCX)

S10 Table. Statistical analysis of dose-response curves of DADLE-stimulated [^{35}S]GTPγS binding. LDM versus 0.025% Brij-58-treated LDM prepared from PTX-treated δ-OR-$G_i1\alpha$ cells.
(DOCX)

S11 Table. Statistical analysis of [^{3}H]DADLE saturation binding curves. LDM versus 0.025% Brij-58-treated LDM prepared from PTX-treated δ-OR-$G_i1\alpha$ cells.
(DOCX)

S12 Table. Statistical analysis of [^{35}S]GTPγS binding. Direct effect of increasing concentrations of Brij-58 in PM isolated from PTX-untreated and PTX-treated δ-OR-$G_i1\alpha$ cells.
(DOCX)

S13 Table. Statistical analysis of dose-response curves of DADLE-stimulated [^{35}S]GTPγS binding. Direct effect of 0.006% Brij-58 in PM.
(DOCX)

S14 Table. Statistical analysis of [^{3}H]DADLE saturation binding curves. Direct effect of 0.006% Brij-58 in PM.
(DOCX)

Author Contributions

Conceived and designed the experiments: PS LR. Performed the experiments: LR MV JB VR. Analyzed the data: LR MV VR JS. Wrote the paper: LR PS.

References

1. Anderson RG. The caveolae membrane system. Annu Rev Biochem. 1998; 67:199–225. doi: 10.1146/annurev.biochem.67.1.199 PMID: 9759488
2. Brown DA, London E. Structure of detergent-resistant membrane domains: does phase separation occur in biological membranes? Biochem Biophys Res Commun. 1997; 240:1–7. doi: 10.1006/bbrc.1997.7575 PMID: 9367871
3. Brown DA, London E. Functions of lipid rafts in biological membranes. Annu Rev Cell Dev Biol. 1998; 14:111–136. doi: 10.1146/annurev.cellbio.14.1.111 PMID: 9891780
4. Brown DA, London E. Structure and origin of ordered lipid domains in biological membranes. J Membr Biol. 1998; 164:103–114. doi: 10.1007/s002329900397 PMID: 9662555
5. Brown DA, London E. Structure and function of sphingolipid- and cholesterol-rich membrane rafts. J Biol Chem. 2000; 275:17221–17224. doi: 10.1074/jbc.R000005200 PMID: 10770957
6. Harder T, Simons K. Caveolae, DIGs, and the dynamics of sphingolipid-cholesterol microdomains. Curr Opin Cell Biol. 1997; 9:534–542. doi: 10.1016/S0955-0674(97)80030-0 PMID: 9261060
7. Lisanti MP, Scherer PE, Tang Z, Sargiacomo M. Caveolae, caveolin and caveolin-rich membrane domains: a signalling hypothesis. Trends Cell Biol. 1994; 4:231–235. doi: 10.1016/0962-8924(94)90114-7 PMID: 14731661
8. Lisanti MP, Scherer PE, Vidugiriene J, Tang Z, Hermanowski-Vosatka A, Tu YH, et al. Characterization of caveolin-rich membrane domains isolated from an endothelial-rich source: implications for human disease. J Cell Biol. 1994; 126:111–126. PMID: 7517942
9. London E, Brown DA. Insolubility of lipids in triton X-100: physical origin and relationship to sphingolipid/cholesterol membrane domains (rafts). Biochim Biophys Acta. 2000; 1508:182–195. doi: 10.1016/S0304-4157(00)00007-1 PMID: 11090825
10. Okamoto T, Schlegel A, Scherer PE, Lisanti MP. Caveolins, a family of scaffolding proteins for organizing "preassembled signaling complexes" at the plasma membrane. J Biol Chem. 1998; 273:5419–5422. doi: 10.1074/jbc.273.10.5419 PMID: 9488658
11. Pike LJ. Lipid rafts: heterogeneity on the high seas. Biochem J. 2004; 378:281–292. doi: 10.1042/BJ20031672 PMID: 14662007
12. Pike LJ. Rafts defined: a report on the Keystone Symposium on Lipid Rafts and Cell Function. J Lipid Res. 2006; 47:1597–1598. doi: 10.1194/jlr.E600002-JLR200 PMID: 16645198
13. Rybin VO, Pak E, Alcott S, Steinberg SF. Developmental changes in beta2-adrenergic receptor signaling in ventricular myocytes: the role of Gi proteins and caveolae microdomains. Mol Pharmacol. 2003; 63:1338–1348. doi: 10.1124/mol.63.6.1338 PMID: 12761344
14. Rybin VO, Xu X, Lisanti MP, Steinberg SF. Differential targeting of beta-adrenergic receptor subtypes and adenylyl cyclase to cardiomyocyte caveolae. A mechanism to functionally regulate the cAMP signaling pathway. J Biol Chem. 2000; 275:41447–41457. doi: 10.1074/jbc.M006951200 PMID: 11006286
15. Shaul PW, Anderson RG. Role of plasmalemmal caveolae in signal transduction. Am J Physiol. 1998; 275:L843–851. PMID: 9815100
16. Simons K, Ikonen E. Functional rafts in cell membranes. Nature. 1997; 387:569–572. doi: 10.1038/42408 PMID: 9177342
17. Smart EJ, Graf GA, McNiven MA, Sessa WC, Engelman JA, Scherer PE, et al. Caveolins, liquid-ordered domains, and signal transduction. Mol Cell Biol. 1999; 19:7289–7304. PMID: 10523618

18. Sargiacomo M, Sudol M, Tang Z, Lisanti MP. Signal transducing molecules and glycosyl-phosphatidylinositol-linked proteins form a caveolin-rich insoluble complex in MDCK cells. J Cell Biol. 1993; 122:789–807. PMID: 8349730

19. Bourova L, Kostrnova A, Hejnova L, Moravcova Z, Moon HE, Novotny J, et al. delta-Opioid receptors exhibit high efficiency when activating trimeric G proteins in membrane domains. J Neurochem. 2003; 85:34–49. doi: 10.1046/j.1471-4159.2003.01667.x PMID: 12641725

20. Song KS, Li S, Okamoto T, Quilliam LA, Sargiacomo M, Lisanti MP. Co-purification and direct interaction of Ras with caveolin, an integral membrane protein of caveolae microdomains. Detergent-free purification of caveolae microdomains. J Biol Chem. 1996; 271:9690–9697. doi: 10.1074/jbc.271.16.9690 PMID: 8621645

21. Song KS, Scherer PE, Tang Z, Okamoto T, Li S, Chafel M, et al. Expression of caveolin-3 in skeletal, cardiac, and smooth muscle cells. Caveolin-3 is a component of the sarcolemma and co-fractionates with dystrophin and dystrophin-associated glycoproteins. J Biol Chem. 1996; 271:15160–15165. doi: 10.1074/jbc.271.25.15160 PMID: 8663016

22. Moravcova Z, Rudajev V, Stohr J, Novotny J, Cerny J, Parenti M, et al. Long-term agonist stimulation of IP prostanoid receptor depletes the cognate G(s)alpha protein in membrane domains but does not change the receptor level. Biochim Biophys Acta. 2004; 1691:51–65. doi: 10.1016/j.bbamcr.2003.12.004 PMID: 15053924

23. Smart EJ, Ying YS, Mineo C, Anderson RG. A detergent-free method for purifying caveolae membrane from tissue culture cells. Proc Natl Acad Sci U S A. 1995; 92:10104–10108. PMID: 7479734

24. Moon HE, Bahia DS, Cavalli A, Hoffmann M, Milligan G. Control of the efficiency of agonist-induced information transfer and stability of the ternary complex containing the delta opioid receptor and the alpha subunit of G(i1) by mutation of a receptor/G protein contact interface. Neuropharmacology. 2001; 41:321–330. doi: 10.1016/S0028-3908(01)00076-4 PMID: 11522323

25. Stohr J, Bourova L, Hejnova L, Ihnatovych I, Novotny J, Svoboda P. Increased baclofen-stimulated G protein coupling and deactivation in rat brain cortex during development. Brain Res Dev Brain Res. 2004; 151:67–73. doi: 10.1016/j.devbrainres.2004.03.014 PMID: 15246693

26. Brejchova J, Sykora J, Dlouha K, Roubalova L, Ostasov P, Vosahlikova M, et al. Fluorescence spectroscopy studies of HEK293 cells expressing DOR-Gi1alpha fusion protein; the effect of cholesterol depletion. Biochim Biophys Acta. 2011; 1808:2819–2829. doi: 10.1016/j.bbamem.2011.08.010 PMID: 21864502

27. Shinitzky M, Barenholz Y. Fluidity parameters of lipid regions determined by fluorescence polarization. Biochim Biophys Acta. 1978; 515:367–394. PMID: 365237

28. Shinitzky M, Inbar M. Microviscosity parameters and protein mobility in biological membranes. Biochim Biophys Acta. 1976; 433:133–149. doi: 10.1016/0005-2736(76)90183-8 PMID: 1260056

29. Sykora J, Bourova L, Hof M, Svoboda P. The effect of detergents on trimeric G-protein activity in isolated plasma membranes from rat brain cortex: correlation with studies of DPH and Laurdan fluorescence. Biochim Biophys Acta. 2009; 1788:324–332. doi: 10.1016/j.bbamem.2008.11.008 PMID: 19071083

30. Kawato S, Kinosita K Jr., Ikegami A. Dynamic structure of lipid bilayers studied by nanosecond fluorescence techniques. Biochemistry. 1977; 16:2319–2324.: PMID: 577184

31. Kinosita K Jr., Ikegami A, Kawato S. On the wobbling-in-cone analysis of fluorescence anisotropy decay. Biophys J. 1982; 37:461–464. doi: 10.1016/S0006-3495(82)84692-4 PMID: 7059650

32. Tolkovsky AM, Levitzki A. Mode of coupling between the beta-adrenergic receptor and adenylate cyclase in turkey erythrocytes. Biochemistry. 1978; 17:3795. PMID: 212105

33. Gross W, Lohse MJ. Mechanism of activation of A2 adenosine receptors. II. A restricted collision-coupling model of receptor-effector interaction. Mol Pharmacol. 1991; 39:524–530. PMID: 2017152

34. Lohse MJ, Klotz KN, Schwabe U. Mechanism of A2 adenosine receptor activation. I. Blockade of A2 adenosine receptors by photoaffinity labeling. Mol Pharmacol. 1991; 39:517–523. PMID: 2017151

35. Stickle D, Barber R. Analysis of receptor-mediated activation of GTP-binding protein/adenylate cyclase using the encounter coupling model. Mol Pharmacol. 1993; 43:397–411. PMID: 8095693

36. Stickle D, Barber R. Collisions and encounters in simulations of receptor/GTP-binding protein interactions via simple diffusion. Biochim Biophys Acta. 1996; 1310:242–250. doi: 10.1016/0167-4889(95)00147-6 PMID: 8611639

37. Remmers AE, Clark MJ, Alt A, Medzihradsky F, Woods JH, Traynor JR. Activation of G protein by opioid receptors: role of receptor number and G-protein concentration. Eur J Pharmacol. 2000; 396:67–75. doi: 10.1016/S0014-2999(00)00212-0 PMID: 10822058

38. Neubig RR. Membrane organization in G-protein mechanisms. FASEB J. 1994; 8:939–946.: PMID: 8088459

39. Neubig RR. Specificity of Receptor–G Protein Coupling: Protein Structure and Cellular Determinants. Semin Neurosci. 1998; 9:189–197. doi: 10.1006/smns.1997.0117

40. Steinberg SF, Brunton LL. Compartmentation of G protein-coupled signaling pathways in cardiac myocytes. Annu Rev Pharmacol Toxicol. 2001; 41:751–773. doi: 10.1146/annurev.pharmtox.41.1.751 PMID: 11264475

41. Anderson RG, Jacobson K. A role for lipid shells in targeting proteins to caveolae, rafts, and other lipid domains. Science. 2002; 296:1821–1825. doi: 10.1126/science.1068886 PMID: 12052946

42. De Luca A, Sargiacomo M, Puca A, Sgaramella G, De Paolis P, Frati G, et al. Characterization of caveolae from rat heart: localization of postreceptor signal transduction molecules and their rearrangement after norepinephrine stimulation. J Cell Biochem. 2000; 77:529–539. doi: 10.1002/(SICI)1097-4644(20000615)77:4<596::AID-JCB7>3.0.CO;2-K PMID: 10771510

43. de Weerd WF, Leeb-Lundberg LM. Bradykinin sequesters B2 bradykinin receptors and the receptor-coupled Galpha subunits Galphaq and Galphai in caveolae in DDT1 MF-2 smooth muscle cells. J Biol Chem. 1997; 272:17858–17866. doi: 10.1074/jbc.272.28.17858 PMID: 9211942

44. Dessy C, Kelly RA, Balligand JL, Feron O. Dynamin mediates caveolar sequestration of muscarinic cholinergic receptors and alteration in NO signaling. EMBO J. 2000; 19:4272–4280. doi: 10.1093/emboj/19.16.4272 PMID: 10944110

45. Feron O, Smith TW, Michel T, Kelly RA. Dynamic targeting of the agonist-stimulated m2 muscarinic acetylcholine receptor to caveolae in cardiac myocytes. J Biol Chem. 1997; 272:17744–17748. doi: 10.1074/jbc.272.28.17744 PMID: 9211926

46. Lasley RD, Narayan P, Uittenbogaard A, Smart EJ. Activated cardiac adenosine A(1) receptors translocate out of caveolae. J Biol Chem. 2000; 275:4417–4421. doi: 10.1074/jbc.275.6.4417 PMID: 10660613

47. Moffett S, Brown DA, Linder ME. Lipid-dependent targeting of G proteins into rafts. J Biol Chem. 2000; 275:2191–2198. doi: 10.1074/jbc.275.3.2191 PMID: 10636925

48. Murthy KS, Makhlouf GM. Heterologous desensitization mediated by G protein-specific binding to caveolin. J Biol Chem. 2000; 275:30211–30219. doi: 10.1074/jbc.M002194200 PMID: 10862762

49. Schwencke C, Okumura S, Yamamoto M, Geng YJ, Ishikawa Y. Colocalization of beta-adrenergic receptors and caveolin within the plasma membrane. J Cell Biochem. 1999; 75:64–72. doi: 10.1002/(SICI)1097-4644(19991001)75:1<64::AID-JCB7>3.0.CO;2-L PMID: 10462705

50. Oh P, Schnitzer JE. Segregation of heterotrimeric G proteins in cell surface microdomains. G(q) binds caveolin to concentrate in caveolae, whereas G(i) and G(s) target lipid rafts by default. Mol Biol Cell. 2001; 12:685–698. PMCID: PMC30973 PMID: 11251080

51. Ostrom RS, Gregorian C, Drenan RM, Xiang Y, Regan JW, Insel PA. Receptor number and caveolar co-localization determine receptor coupling efficiency to adenylyl cyclase. J Biol Chem. 2001; 276:42063–42069. doi: 10.1074/jbc.M105348200 PMID: 11533056

52. Ostrom RS, Insel PA. The evolving role of lipid rafts and caveolae in G protein-coupled receptor signaling: implications for molecular pharmacology. Br J Pharmacol. 2004; 143:235–245. doi: 10.1038/sj.bjp.0705930 PMID: 15289291

53. Ostrom RS, Post SR, Insel PA. Stoichiometry and compartmentation in G protein-coupled receptor signaling: implications for therapeutic interventions involving G(s). J Pharmacol Exp Ther. 2000; 294:407–412. PMID: 10900212

54. Sabourin T, Bastien L, Bachvarov DR, Marceau F. Agonist-induced translocation of the kinin B(1) receptor to caveolae-related rafts. Mol Pharmacol. 2002; 61:546–553. doi: 10.1124/mol.61.3.546 PMID: 11854434

55. Ushio-Fukai M, Hilenski L, Santanam N, Becker PL, Ma Y, Griendling KK, et al. Cholesterol depletion inhibits epidermal growth factor receptor transactivation by angiotensin II in vascular smooth muscle cells: role of cholesterol-rich microdomains and focal adhesions in angiotensin II signaling. J Biol Chem. 2001; 276:48269–48275. doi: 10.1074/jbc.M105901200 PMID: 11585822

56. Allen JA, Halverson-Tamboli RA, Rasenick MM. Lipid raft microdomains and neurotransmitter signalling. Nat Rev Neurosci. 2007; 8:128–140. doi: 10.1038/nrn2059 PMID: 17195035

57. Huang P, Xu W, Yoon SI, Chen C, Chong PL, Liu-Chen LY. Cholesterol reduction by methyl-beta-cyclodextrin attenuates the delta opioid receptor-mediated signaling in neuronal cells but enhances it in non-neuronal cells. Biochem Pharmacol. 2007; 73:534–549. doi: 10.1016/j.bcp.2006.10.032 PMID: 17141202

58. Monastyrskaya K, Hostettler A, Buergi S, Draeger A. The NK1 receptor localizes to the plasma membrane microdomains, and its activation is dependent on lipid raft integrity. J Biol Chem. 2005; 280:7135–7146. doi: 10.1074/jbc.M405806200 PMID: 15590676

59. Savi P, Zachayus JL, Delesque-Touchard N, Labouret C, Herve C, Uzabiaga MF, et al. The active metabolite of Clopidogrel disrupts P2Y12 receptor oligomers and partitions them out of lipid rafts. Proc Natl Acad Sci U S A. 2006; 103:11069–11074. doi: 10.1073/pnas.0510446103 PMID: 16835302

60. Xu W, Yoon SI, Huang P, Wang Y, Chen C, Chong PL, et al. Localization of the kappa opioid receptor in lipid rafts. J Pharmacol Exp Ther. 2006; 317:1295–1306. doi: 10.1124/jpet.105.099507 PMID: 16505160

61. Zhao H, Loh HH, Law PY. Adenylyl cyclase superactivation induced by long-term treatment with opioid agonist is dependent on receptor localized within lipid rafts and is independent of receptor internalization. Mol Pharmacol. 2006; 69:1421–1432. doi: 10.1124/mol.105.020024 PMID: 16415176

62. Zheng H, Pearsall EA, Hurst DP, Zhang Y, Chu J, Zhou Y, et al. Palmitoylation and membrane cholesterol stabilize mu-opioid receptor homodimerization and G protein coupling. BMC Cell Biol. 2012; 13:6. doi: 10.1186/1471-2121-13-6 PMID: 22429589

63. Alves ID, Salamon Z, Hruby VJ, Tollin G. Ligand modulation of lateral segregation of a G-protein-coupled receptor into lipid microdomains in sphingomyelin/phosphatidylcholine solid-supported bilayers. Biochemistry. 2005; 44:9168–9178. doi: 10.1021/bi050207a PMID: 15966741

64. Salamon Z, Cowell S, Varga E, Yamamura HI, Hruby VJ, Tollin G. Plasmon resonance studies of agonist/antagonist binding to the human delta-opioid receptor: new structural insights into receptor-ligand interactions. Biophys J. 2000; 79:2463–2474. doi: 10.1016/S0006-3495(00)76489-7 PMID: 11053123

65. Jensen MO, Mouritsen OG. Lipids do influence protein function-the hydrophobic matching hypothesis revisited. Biochim Biophys Acta. 2004; 1666:205–226. doi: 10.1016/j.bbamem.2004.06.009 PMID: 15519316

66. Lee AG. How lipids affect the activities of integral membrane proteins. Biochim Biophys Acta. 2004; 1666:62–87. doi: 10.1016/j.bbamem.2004.05.012 PMID: 15519309

67. Epand RF, Thomas A, Brasseur R, Vishwanathan SA, Hunter E, Epand RM. Juxtamembrane protein segments that contribute to recruitment of cholesterol into domains. Biochemistry. 2006; 45:6105–6114. doi: 10.1021/bi060245+ PMID: 16681383

68. Epand RM, Sayer BG, Epand RF. Caveolin scaffolding region and cholesterol-rich domains in membranes. J Mol Biol. 2005; 345:339–350. doi: 10.1016/j.jmb.2004.10.064 PMID: 15571726

69. Cvejic S, Devi LA. Dimerization of the delta opioid receptor: implication for a role in receptor internalization. J Biol Chem. 1997; 272:26959–26964. doi: 10.1074/jbc.272.43.26959 PMID: 9341132

70. George SR, Fan T, Xie Z, Tse R, Tam V, Varghese G, et al. Oligomerization of mu- and delta-opioid receptors. Generation of novel functional properties. J Biol Chem. 2000; 275:26128–26135. doi: 10.1074/jbc.M000345200 PMID: 10842167

71. Gomes I, Jordan BA, Gupta A, Trapaidze N, Nagy V, Devi LA. Heterodimerization of mu and delta opioid receptors: A role in opiate synergy. J Neurosci. 2000; 20:RC110. 20004736 [pii] PMID: 11069979

72. He L, Fong J, von Zastrow M, Whistler JL. Regulation of opioid receptor trafficking and morphine tolerance by receptor oligomerization. Cell. 2002; 108:271–282. doi: 10.1016/S0092-8674(02)00613-X PMID: 11832216

73. Jordan BA, Devi LA. G-protein-coupled receptor heterodimerization modulates receptor function. Nature. 1999; 399:697–700. doi: 10.1038/21441 PMID: 10385123

74. Lohse MJ. Dimerization in GPCR mobility and signaling. Curr Opin Pharmacol. 2010; 10:53–58. doi: 10.1016/j.coph.2009.10.007 PMID: 19910252

75. Manglik A, Kruse AC, Kobilka TS, Thian FS, Mathiesen JM, Sunahara RK, et al. Crystal structure of the mu-opioid receptor bound to a morphinan antagonist. Nature. 2012; 485:321–326. doi: 10.1038/nature10954 PMID: 22437502

76. McVey M, Ramsay D, Kellett E, Rees S, Wilson S, Pope AJ, et al. Monitoring receptor oligomerization using time-resolved fluorescence resonance energy transfer and bioluminescence resonance energy transfer. The human delta-opioid receptor displays constitutive oligomerization at the cell surface, which is not regulated by receptor occupancy. J Biol Chem. 2001; 276:14092–14099. doi: 10.1074/jbc.M008902200 PMID: 11278447

77. Ramsay D, Kellett E, McVey M, Rees S, Milligan G. Homo- and hetero-oligomeric interactions between G-protein-coupled receptors in living cells monitored by two variants of bioluminescence resonance energy transfer (BRET): hetero-oligomers between receptor subtypes form more efficiently than between less closely related sequences. Biochem J. 2002; 365:429–440. doi: 10.1042/BJ20020251 PMID: 11971762